Zeolitic Diagenesis of Tuffs in Miocene Lacustrine Rocks near Harney Lake, Harney County, Oregon

U.S. GEOLOGICAL SURVEY BULLETIN 2108

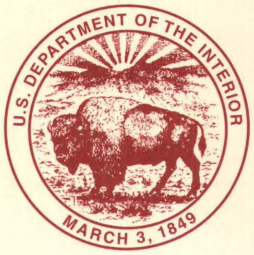

AVAILABILITY OF BOOKS AND MAPS OF THE U.S. GEOLOGICAL SURVEY

Instructions on ordering publications of the U.S. Geological Survey, along with prices of the last offerings, are given in the current-year issues of the monthly catalog "New Publications of the U.S. Geological Survey." Prices of available U.S. Geological Survey publications released prior to the current year are listed in the most recent annual "Price and Availability List." Publications that may be listed in various U.S. Geological Survey catalogs (**see back inside cover**) but not listed in the most recent annual "Price and Availability List" may no longer be available.

Reports released through the NTIS may be obtained by writing to the National Technical Information Service, U.S. Department of Commerce, Springfield, VA 22161; please include NTIS report number with inquiry.

Order U.S. Geological Survey publications **by mail** or **over the counter** from the offices listed below.

BY MAIL

Books

Professional Papers, Bulletins, Water-Supply Papers, Techniques of Water-Resources Investigations, Circulars, publications of general interest (such as leaflets, pamphlets, booklets), single copies of Earthquakes & Volcanoes, Preliminary Determination of Epicenters, and some miscellaneous reports, including some of the foregoing series that have gone out of print at the Superintendent of Documents, are obtainable by mail from

U.S. Geological Survey, Map Distribution
Box 25286, MS 306, Federal Center
Denver, CO 80225

Subscriptions to periodicals (Earthquakes & Volcanoes and Preliminary Determination of Epicenters) can be obtained ONLY from the

Superintendent of Documents
Government Printing Office
Washington, DC 20402

(Check or money order must be payable to Superintendent of Documents.)

Maps

For maps, address mail orders to

U. S. Geological Survey, Map Distribution
Box 25286, Bldg. 810, Federal Center
Denver, CO 80225

Residents of Alaska may order maps from

U.S. Geological Survey, Earth Science Information Center
101 Twelfth Ave., Box 12
Fairbanks, AK 99701

OVER THE COUNTER

Books and Maps

Books and maps of the U.S. Geological Survey are available over the counter at the following U.S. Geological Survey offices, all of which are authorized agents of the Superintendent of Documents.

- **ANCHORAGE, Alaska**–Rm. 101, 4230 University Dr.
- **LAKEWOOD, Colorado**–Federal Center, Bldg. 810
- **MENLO PARK, California**–Bldg. 3, Rm. 3128, 345 Middlefield Rd.
- **RESTON, Virginia**–USGS National Center, Rm. 1C402, 12201 Sunrise Valley Dr.
- **SALT LAKE CITY, Utah**–Federal Bldg., Rm. 8105, 125 South State St.
- **SPOKANE, Washington**–U.S. Post Office Bldg., Rm. 135, West 904 Riverside Ave.
- **WASHINGTON, D.C.**–Main Interior Bldg., Rm. 2650, 18th and C Sts., NW.

Maps Only

Maps may be purchased over the counter at the following U.S. Geological Survey offices:

- **FAIRBANKS, Alaska**–New Federal Bldg, 101 Twelfth Ave.
- **ROLLA, Missouri**–1400 Independence Rd.
- **STENNIS SPACE CENTER, Mississippi**–Bldg. 3101

Zeolitic Diagenesis of Tuffs in Miocene Lacustrine Rocks near Harney Lake, Harney County, Oregon

By Richard A. Sheppard

U.S. GEOLOGICAL SURVEY BULLETIN 2108

Silicic vitric tuffs east of Harney Lake are altered chiefly to clinoptilolite with or without other zeolites such as analcime, chabazite, erionite, mordenite, and phillipsite

UNITED STATES GOVERNMENT PRINTING OFFICE, WASHINGTON : 1994

U.S. DEPARTMENT OF THE INTERIOR
BRUCE BABBITT, Secretary

U.S. GEOLOGICAL SURVEY
Gordon P. Eaton, Director

Published in the Central Region, Denver, Colorado
Manuscript approved for publication July 28, 1994
Edited by Judith Stoeser
Graphics and photocomposition by Mari L. Kauffmann
Tables typeset by Judith Stoeser

For sale by U.S. Geological Survey, Map Distribution
Box 25286, MS 306, Federal Center
Denver, CO 80225

Library of Congress Cataloging-in-Publication Data

Sheppard, Richard A.
Zeolitic diagenesis of tuffs in Miocene lacustrine rocks near Harney Lake, Harney County, Oregon / by Richard A. Sheppard.
p. cm.—(U.S. Geological Survey bulletin ; 2108)
Includes bibliographical references.
Supt. of Docs. no. : I 19.3:2108
1. Zeolities—Oregon—Harney County. 2. Rocks, Sedimentary—Oregon—Harney County. 3. Volcanic ash, tuff, etc.—Oregon—Harney County. 4. Diagenesis—Oregon—Harney County. 5. Geology, Stratigraphic—Miocene. 6. Geology—Oregon—Harney County. I. Title. II. Series.
QE75.B9 no. 2108
[QE39.Z5]
557.3 s—dc20 94–23426
[552′.5′0979595] CIP

CONTENTS

FIGURES

TABLES

Zeolitic Diagenesis of Tuffs in Miocene Lacustrine Rocks near Harney Lake, Harney County, Oregon

By Richard A. Sheppard

ABSTRACT

Tuffaceous sedimentary rocks crop out in a dissected upland area of about 72 km^2, south of Narrows and east of Harney Lake, Harney County, Oregon. These rocks are part of the now-abandoned Danforth Formation, which also included interstratified ash-flow tuffs and local basalt flows. Three regionally extensive ash-flow tuffs, from oldest to youngest, the Devine Canyon, Prater Creek, and Rattlesnake Ash-flow Tuffs, recently were assigned formal names, but the tuffaceous sedimentary rocks and interstratified basalt flows still remain unnamed. Zeolitic tuffaceous rocks near Harney Lake are between the Devine Canyon and Rattlesnake Ash-flow Tuffs and include a local nonwelded facies of the Prater Creek Ash-flow Tuff. An age of 9.3–6.5 Ma for these sedimentary rocks is constrained by the dated Devine Canyon and Rattlesnake Ash-flow Tuffs. The tuffaceous sedimentary sequence has a maximum thickness of about 120 m but thins southward to about 5 m.

The tuffaceous sedimentary rocks are chiefly lacustrine but are locally fluviatile, particularly near the southern margin of the depositional basin. Lacustrine rocks are most common at the northern and western parts of the studied area. Rock types include mudstone, siltstone, sandstone, tuff, chert, limestone, and rare dolomite. Some of the chert is a variety known as Magadi type that is present only in deposits of alkaline, saline lakes. Except for the chert, all the rocks originally contained a rhyolitic vitroclastic component. The abundance of discrete tuffs and the abundance of vitroclastic material in the tuffaceous rocks decrease from north to south. Epiclastic grains in the tuffaceous rocks are chiefly alkali feldspar, plagioclase, quartz, and volcanic rock fragments, and these components increase in abundance from north to south and, locally, from west to east. Although the abundance of unaltered glass in the tuffaceous rocks increases toward the southern margin of the basin, tuffs consisting entirely of unaltered vitric material have not been recognized. Some tuff in the southern part of the area consists of as much as 90 percent unaltered glass, but most tuff, including the interstratified nonwelded ash-flow tuff, lacks glass or contains minor relict glass and variable amounts of authigenic smectite, zeolites, and opal-CT.

The sequence of crystallization of authigenic zeolites and coexisting silicate minerals in the tuffaceous rocks was determined by thin section examination and scanning electron microscopy. Smectite was generally the first mineral to form in the tuffaceous rocks, and it locally coats vitric material. The zeolites are commonly perched on a mat of smectite, although some chabazite and erionite were observed to be in direct contact with pitted glass shards that lacked a smectite coating. Chabazite and phillipsite probably were the first zeolites to crystallize. Then, from early to late, the sequence is clinoptilolite, mordenite, and erionite. Local slight dissolution of clinoptilolite and chabazite occurred prior to the crystallization of erionite, and slight dissolution of clinoptilolite occurred prior to the crystallization of mordenite. Analcime was the last zeolite to crystallize, and it replaced smectite, clinoptilolite, erionite, and phillipsite and probably the other zeolites. The authigenic potassium feldspar probably was the last silicate mineral to form in the tuffaceous rocks. Potassium feldspar was observed to have replaced clinoptilolite and analcime, but it probably also locally replaced all the pre-existing authigenic silicate minerals.

The zeolites and coexisting silicate minerals in the tuffaceous rocks formed during diagenesis by dissolution of silicic glass by pore waters of various compositions. Differences in pH and salinity of the pore waters were inherited from water that was trapped in the tuffaceous rocks during deposition in an ancient lake. The pore water ranged from dilute and almost neutral in nearshore and inlet parts of the lake to saline, alkaline brine having a pH of 9 or greater in the central part of the lake. The northward and westward transition of authigenic minerals from relict glass to zeolites and then to potassium feldspar reflects this variation in the composition of the trapped lake water. Those parts of the tuffaceous rocks that still contain vitric material were probably deposited in relatively fresh water near the major inlet of the ancient lake. Farther basinward, zeolites and potassium feldspar crystallized in the tuffaceous rocks and the interstratified ash-flow tuffs because of the increased pH and salinity of the lake water. Although potassium feldspar presumably

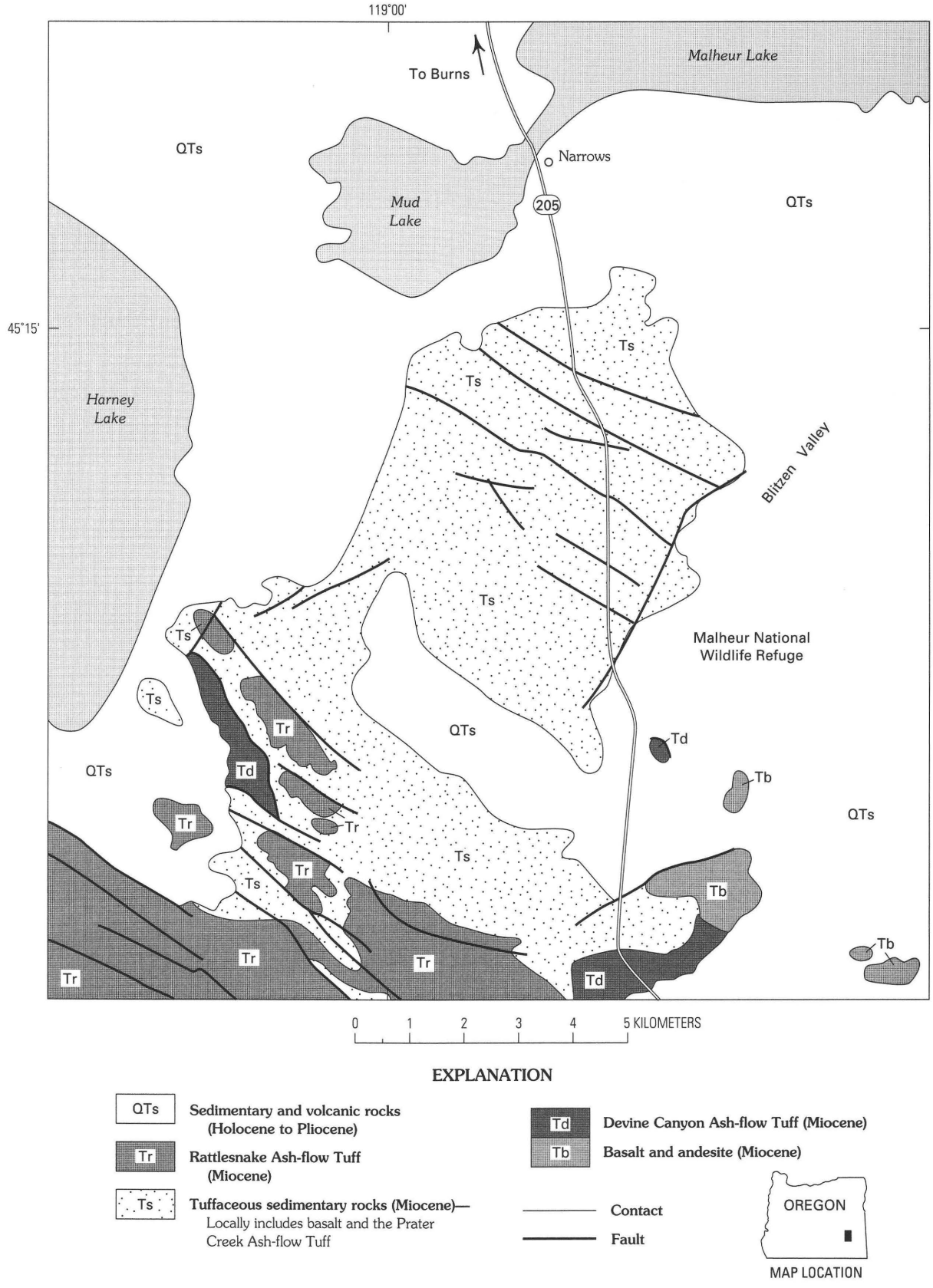

Figure 1. Generalized geologic map showing distribution of Miocene tuffaceous sedimentary rocks and ash-flow tuffs east of Harney Lake, Oregon. Modified from Greene and others (1972).

could have formed directly from material dissolved from the silicic glass by the pore water, there is no evidence that this occurred. The potassium feldspar in the tuffaceous rocks formed chiefly from precursor zeolites.

INTRODUCTION

Miocene tuffaceous sedimentary rocks east of Harney Lake, Harney County, Oregon (fig. 1), and about 40 km south of Burns contain a large, potentially commercial zeolite deposit. This part of southeastern Oregon is in the southeastern part of the High Lava Plains physiographic province, a region of high plateaus and few permanent streams, about 1,200–1,800 m above sea level. The upland east of Harney Lake is a dissected part of Harney Basin and is characterized by badlands and benches. Harney Basin covers about 13,700 km^2 in Harney and Grant Counties (Walker, 1979). Rocks of the region are mainly flat lying to gently tilted Neogene and Quaternary volcanic and continental sedimentary rocks. Numerous closely spaced, en echelon normal faults cut the Cenozoic rocks but have only slight (commonly 10–100 m) displacements (Walker and Nolf, 1981). The zeolites and associated authigenic minerals are in an unnamed Miocene sequence of alluvial and lacustrine volcaniclastic rocks that had been part of the now-abandoned Danforth Formation (Piper and others,1939).

PREVIOUS WORK

The earliest geological investigations of the Harney Basin were reported by Russell (1884), but Piper and others (1939) separated the Cenozoic sedimentary and volcanic sequence into several units and prepared a geologic map. One of these mapped units was the now-abandoned Danforth Formation (Piper and others, 1939), assigned a Pliocene age according to the then-existing geologic time scale. The Danforth Formation, as originally described, consisted of intertonguing continental tuffaceous sedimentary rocks, basaltic breccia and flows, and rhyolitic tuff-breccia and flows. Subsequent geologic mapping and petrologic studies showed that the rhyolitic tuff-breccia and flows were widespread, mappable ash-flow tuffs (Walker and Swanson, 1968; Greene, 1973; Parker, 1974). During their geologic reconnaissance of the Burns 1°×2° quadrangle, Greene and others (1972) mapped a unit of tuffaceous sedimentary rocks that includes the zeolite-bearing tuffs of the present investigation. Walker (1979) abandoned the Danforth Formation and formally named three regionally extensive ash-flow tuffs, from oldest to youngest, the Devine Canyon, Prater Creek, and Rattlesnake Ash-flow Tuffs. The tuffaceous sedimentary rocks and interstratified basaltic rocks remain unnamed.

Zeolites were discovered in the region in 1959 by H.M. Wharton during an exploration program conducted throughout the western United States for the Linde Division of Union Carbide Corporation, but the finding of clinoptilolite, erionite, and mordenite in tuffs near Harney Lake was not published until much later (Mumpton, 1984). As part of an investigation of mineral resources near Harney and Malheur Lakes, Walker and Swanson (1968) reported significant concentrations of clinoptilolite, erionite, and phillipsite in the tuffaceous sedimentary rocks. Walker and Swanson (1968, p. L11) also recognized that some tuffs contain as much as 60 percent diagenetic potassium feldspar. Commercial interest in the zeolites near Harney Lake began in 1975 when Anaconda Minerals Company filed claims east of Harney Lake and south of Narrows. Claims covering much of the zeolite-bearing tuffs south of the Anaconda claims were filed in 1979 by Occidental Minerals Company. Drilling and evaluation of the zeolite deposit by both companies continued into the 1980's. Since then, several other companies, including PDZ Corporation, Tenneco Specialty Minerals, Steelhead Specialty Minerals, East West Minerals, Inc., and New Gold, Inc., have had an interest in part or all of the properties previously held by Anaconda and Occidental. As of 1993, only Geo-Environmental Resources, Inc., appeared to have an active interest in the zeolites. In spite of the extensive drilling and evaluation over the years, only a minor tonnage of clinoptilolite-rich tuff has been produced for testing. Inasmuch as the Harney Lake area contains a significant deposit of clinoptilolite-rich tuffs (probably in excess of 100 million tons) that could be mined by open-pit methods, the zeolite has a high potential for future economic exploitation.

The only published studies on the distribution and genesis of zeolites and associated authigenic minerals in the tuffaceous sedimentary rocks near Harney Lake are those of Walker and Swanson (1968), Holmes (1990, p. 84), and Sheppard (1993). Although the three reports are brief, the authors all recognized that the zeolites resulted from diagenetic alteration of silicic ash in a closed hydrologic system.

SCOPE OF PRESENT INVESTIGATION

After a brief reconnaissance of the alteration of the Miocene tuffaceous rocks near Harney Lake in 1987, I concentrated on an area chiefly south of Narrows (fig. 1) and between Harney Lake and the Blitzen Valley. Almost 300 samples of fresh and diagenetically altered tuffs and tuffaceous sediments from this area were collected and studied during 1988–1991 (fig. 2). These Miocene tuffaceous rocks were chosen for detailed study for the following reasons: (1) the sequence includes numerous tuffs that are both fresh (unaltered) and altered to a variety of authigenic silicate minerals, (2) the sequence of rocks was subjected to relatively shallow burial and was affected by only slight

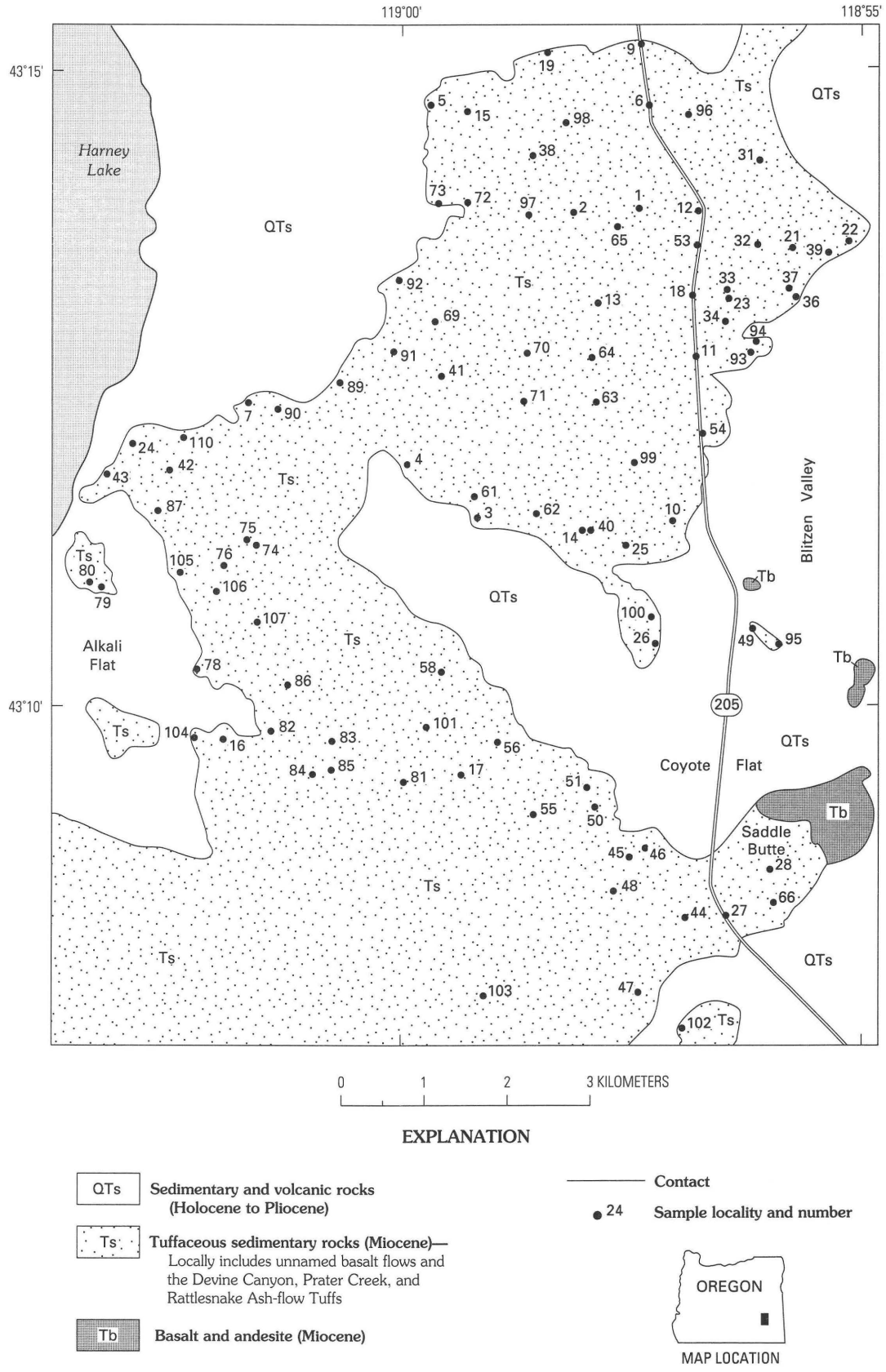

Figure 2. Map showing sample localities in the Miocene tuffaceous rocks east of Harney Lake, Oregon. Mineralogic composition of samples, as estimated from X-ray diffractometer patterns, is given in the appendix.

deformation and no obvious hydrothermal alteration, (3) surface exposures are good, and (4) interbedded ash-flow tuffs provided a means of stratigraphic correlation throughout the area. Objectives of this investigation were to delineate the pattern of zeolite alteration, to characterize the authigenic minerals and their paragenetic relationships, and to suggest a possible origin for the zeolites and associated silicate minerals in the tuffaceous rocks.

LABORATORY METHODS

The mineralogy of bulk samples was determined by X-ray diffraction analysis. Samples were first ground to a powder and then packed in aluminum sample holders, exposed to copper radiation, and scanned at 2° 2Θ per minute over a range of 2°–40° 2Θ. Relative abundances of the minerals were visually estimated from the diffractometer patterns following the procedure outlined by Sheppard and Gude (1968, p. 2–3). Estimates are probably less reliable for samples containing glass or opal-CT because these materials yield rather poor X-ray records.

Textures and paragenetic relationships of the diagenetic minerals were examined in thin sections and immersion oil mounts by transmitted-light microscopy and by scanning electron microscopy of freshly broken fragments. Samples to be studied by scanning electron microscopy were coated with carbon and then recoated with a film of gold (about 300 Å thick) just prior to examination.

The chemical compositions of bulk samples of almost monomineralic zeolitic tuffs and glass-shard separates were determined by standard X-ray fluorescence analysis. The H_2O content was determined by weight loss on ignition at 925°C. A semiquantitative energy-dispersive X-ray unit, attached to the scanning electron microscope, was used to determine the Si:Al ratios of selected zeolites. Glass-shard separates were prepared by crushing the tuff and then disaggregating it in an ultrasonic bath. The glass shards were then concentrated by repeated centrifuging in a heavy-liquid mixture of bromoform and acetone.

Acknowledgments.—Appreciation is expressed to those in the U.S. Geological Survey who provided technical assistance during this investigation; Gary L. Skipp performed separations of zeolites and glass shards in the laboratory, and James M. Nishi patiently provided guidance during my use of the scanning electron microscope. I also thank Richard W. Knostman of Nathrop, Colorado, for supplying unpublished drillhole data on zeolitic tuffs from the northern part of the area.

GEOLOGIC SETTING

Harney Basin is a structurally controlled basin underlain chiefly by volcanic and volcaniclastic rocks. It apparently began to evolve as a large structural downwarp and as a site of sedimentation during middle or late Miocene time (Walker, 1979). Much of the structural collapse associated with the formation of the basin probably was the result of the eruption of large volumes of basaltic and rhyolitic material from large collapse calderas within the basin (Walker and Nolf, 1981). The upper Cenozoic rocks of Harney Basin are a complexly intertongued and locally faulted assemblage of andesite, basaltic flows and volcaniclastic rocks, minor rhyolite domes and flows, and rhyolitic air-fall and ash-flow tuffs and tuffaceous sedimentary rocks.

Zeolitic tuffaceous rocks near Harney Lake and south of Narrows are part of the now-abandoned Danforth Formation (Piper and others, 1939). These upper Miocene tuffaceous rocks are stratigraphically between the Devine Canyon and Rattlesnake Ash-flow Tuffs and are interstratified with a nonwelded facies of the Prater Creek Ash-flow Tuff. The Devine Canyon Ash-flow Tuff unconformably overlies Miocene andesite and basalt. Locally, a sequence of tuffaceous sedimentary rocks separates the Devine Canyon Ash-flow Tuff from the underlying unit of andesite and basalt (Walker, 1979). The Rattlesnake Ash-flow Tuff is unconformably overlain by the Pliocene Harney Formation. The ash-flow tuffs and tuffaceous sedimentary rocks commonly dip 8°–20° NE. and are cut by numerous northwest-trending faults of slight displacement. Near the faults, the rocks locally dip to the southwest.

STRATIGRAPHY AND LITHOLOGY OF THE TUFFACEOUS SEDIMENTARY ROCKS

The Miocene tuffaceous sedimentary rocks (including the locally nonwelded facies of the Prater Creek Ash-flow Tuff) between the Devine Canyon and Rattlesnake Ash-flow Tuffs are chiefly lacustrine but are locally fluviatile, particularly near the southern part of the depositional basin. Lacustrine rocks are most common in the northern and western parts of the area. The sedimentary rocks consist chiefly of mudstone, siltstone, sandstone, and numerous volcanic ash beds or tuffs. For convenience throughout the remainder of this report, the volcanic ashes are referred to as tuffs even though they are relatively unconsolidated and unaltered. Relatively thin (less than 40 cm thick) carbonate and chert beds are conspicuous but not common. In addition to the numerous discrete tuffs, most epiclastic rocks have a tuffaceous component. The abundance of discrete tuffs and the abundance of vitroclastic material in the tuffaceous rocks decreases from north to south. Epiclastic grains in the tuffaceous rocks are chiefly alkali feldspar, plagioclase, quartz, and volcanic rock fragments and minor biotite, hornblende, and clinopyroxene, and these components increase in abundance from north to south and, locally, from west to east.

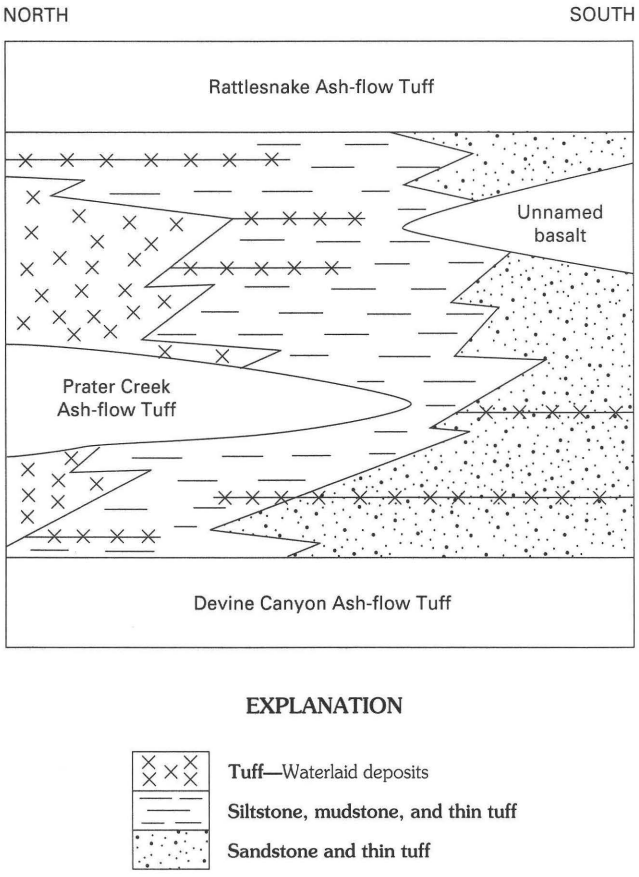

Figure 3. Schematic north-south cross section showing lithologic relationships in Miocene tuffaceous rocks between the Devine Canyon Ash-flow Tuff and the Rattlesnake Ash-flow Tuff, east of Harney Lake, Oregon.

This tuffaceous sedimentary sequence has a maximum thickness of about 120 m but thins southward to about 5 m approximately 22 km south of Narrows. The complete stratigraphic section is nowhere exposed. Less than 50 m of tuffaceous sedimentary rocks generally crop out at any given exposure, but the common exposed section is much less than 50 m thick. Figure 3 is a diagrammatic north-south cross section that shows the lithologic relationships in the Miocene tuffaceous rocks between the Devine Canyon Ash-flow Tuff and the Rattlesnake Ash-flow Tuff. Unless an interstratified ash-flow tuff is present, correlation of the tuffaceous sedimentary rocks from outcrop to outcrop is difficult because of significant changes in sedimentary facies over a short distance and because of faulting and erosion.

An age of 9.3–6.5 Ma for these tuffaceous sedimentary rocks is constrained by the dated Devine Canyon and Rattlesnake Ash-flow Tuffs (Walker, 1979). The Prater Creek Ash-flow Tuff has an age of about 8.4 Ma according to Walker (1979).

Fossil ostracodes, snails, and plant debris were recognized in the tuffaceous sedimentary rocks during this investigation. A special effort was made to collect ostracode-bearing samples with the hope of using the ostracodes to reconstruct the water chemistry of the depositional environment. Unfortunately, most samples contained only molds or casts of ostracodes, and the ostracodes could not be identified at any taxonomic level. Unidentified fossil snails were recognized only from the southern part of the area where they are in strata that contain relict vitric material.

SANDSTONE

Sandstone is generally gray, yellowish gray, or yellowish brown and is highly variable in grain size, thickness, and induration. Most commonly, sandstone is medium to coarse grained and medium to thick bedded. Crossbedding is locally common, and the dips of foresets near the southern part of the area indicate a northerly (basinward) transport direction. Cementation is common; cements are chiefly smectite, clinoptilolite, erionite (fig. 4), and calcite, but phillipsite, opal-CT, cristobalite, and quartz have also been recognized.

The framework constituents of sandstone consist of varying amounts of mineral grains, lithic fragments, and vitroclastic (or altered vitroclastic) particles. Sorting is commonly poor, and the clasts are generally angular to subrounded. Detrital mineral grains are chiefly quartz, plagioclase, and alkali feldspar and lesser amounts of biotite, hornblende, clinopyroxene, and zircon. Some hornblende and clinopyroxene grains show dissolution features. Lithic grains are mostly silicic volcanic rocks. The tuffaceous component commonly makes up 20–60 percent of the framework and varies from fresh to completely altered.

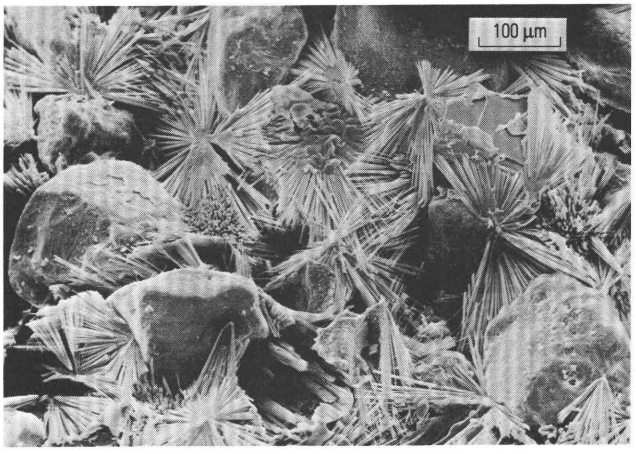

Figure 4. Scanning electron micrograph of tuffaceous sandstone showing radial aggregates of acicular erionite that cemented detrital grains. Locality 17, figure 2; sample HL–17A.

SILTSTONE AND MUDSTONE

These fine-grained detrital rocks in the Harney Lake area are generally deeply weathered and commonly do not crop out. Both siltstone and mudstone are medium to thick bedded and brown, green, or gray and have an earthy luster. Most mudstone contains, in addition to clay minerals, detrital sand grains and authigenic minerals. Angular to subrounded detrital mineral grains commonly make up about 10–40 percent of the mudstone and are the same suite that is in the sandstone and siltstone. Authigenic minerals include analcime, clinoptilolite, erionite, phillipsite, and potassium feldspar.

MAGADI-TYPE CHERT

Chert that formed from magadiite ($NaSi_7O_{13}OH)_3 \cdot 3H_2O$) or other hydrous sodium silicate minerals was first described by Eugster (1967), who observed it in upper Pleistocene lacustrine deposits at Lake Magadi, Kenya. Since then, this distinctive chert of inorganic origin has been recognized in many lacustrine deposits of Jurassic to Pleistocene age, particularly in the western United States (Sheppard and Gude, 1986). Magadi-type chert in the tuffaceous rocks near Harney Lake is present as nodules and thin plates that are commonly 2–10 cm long. The chert is light gray, dense, and milky to translucent; it generally has a thin (0.5–2 mm), soft, white coating or rind. A characteristic surface reticulation has led rock collectors and lapidaries to describe the chert as "snakeskin agate." X-ray diffraction patterns of the Magadi-type chert show that it consists of variable amounts of quartz and moganite (Heaney and others, 1992). Most of the Magadi-type chert recognized in the tuffaceous rocks is in the upper part of the stratigraphic section and in the northern part of the area.

BASALT FLOWS AND BASALTIC TUFF

Two or more flows of basalt that aggregate 13–35 m in thickness are interbedded with the upper part of the tuffaceous sedimentary rocks in the southeastern part of the area. The upper part of Saddle Butte consists entirely of basalt. Where fresh the basalt is black, but where weathered it is brown. The basalt consists of glomeroporphyritic clots of olivine in a holocrystalline groundmass of calcic plagioclase laths, ophitic clinopyroxene, olivine, and minor opaque minerals. Much of the olivine shows an unidentified, brown alteration material (iddingsite?) along fractures.

Basaltic tuff is present locally beneath the basalt flows and is 6 cm–1.6 m thick. The tuff is brown, coarse grained, poorly sorted, and poorly indurated. It consists almost entirely of angular fragments of vesicular, glassy basalt that are 0.5–8 mm long. Most of the basaltic clasts show some alteration to smectite, zeolites, and calcite. Phillipsite, chabazite, and analcime have been identified, and phillipsite commonly is present as a cement. The genesis and the distribution of alteration minerals in the basaltic tuff were studied but will not be discussed further herein.

TUFF

Discrete silicic, vitric tuff or its altered equivalents makes up about 4–32 percent of the stratigraphic section and probably is most abundant in the northern part of the area. The tuffs or tuff units are about 2 cm to 45 m thick. Thin tuff units are commonly single beds, but most tuff units thicker than 40 cm comprise more than one bed. Individual units of either single-bedded or multiple-bedded tuff are commonly graded, being coarser at the base. Some thin tuff units and the lower parts of thick tuff units are the result of ash falls directly into the ancient lake. Other tuff (particularly the upper parts of thick tuff units) consists of reworked vitroclastic material mixed with epiclastic grains.

Tuff consisting entirely of unaltered vitric material has not been recognized, although some tuff in the southern part of the area consists of as much as 90 percent unaltered glass. The relatively unaltered tuff is light gray, and the vitric material has a characteristic vitreous luster. This tuff is very friable and easily disaggregated with the fingers. Natural exposures are poor; therefore, thin fresh tuff could easily be overlooked. The lower contact of a tuff generally is sharp, whereas the upper contact is commonly gradational into the overlying rock, regardless of lithology. Ripple marks, laminations, crossbedding, and contorted bedding are present but rare.

The silicic tuff is vitric but contains varying amounts of crystal and rock fragments. Most silicic tuff is fine to medium grained. Vitric particles consist of platy bubble-wall shards formed from the walls of relatively large, broken bubbles and pumice shards that contain small elongated bubbles. Platy bubble-wall shards generally predominate. The relict glass shards commonly show obvious dissolution features including pitting and corrosion (fig. 5). The index of refraction of unaltered shards ranges from 1.495 to 1.503. Angular crystal and rock fragments commonly make up 1–10 percent of the silicic tuff. Pyrogenic crystals consist of quartz, sodic plagioclase, alkali feldspar, hornblende, clinopyroxene, and zircon. The rock fragments are chiefly silicic lavas. Mineral grains of epiclastic origin are biotite and epidote.

Chemical analyses of unaltered shards separated from two vitric tuffs indicate a rhyolitic composition (table 1). These analyses are similar to an analysis (sample 3, table 1) of the basal part of the Rattlesnake Ash-flow Tuff where it is vitric, unaltered, and nonwelded. Although the vitric material does not contain any authigenic minerals, the high (about 4–6 percent) H_2O content is evidence that even the freshest

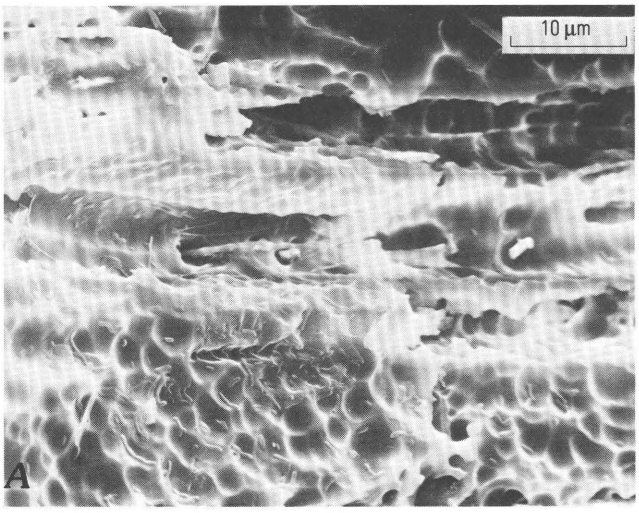

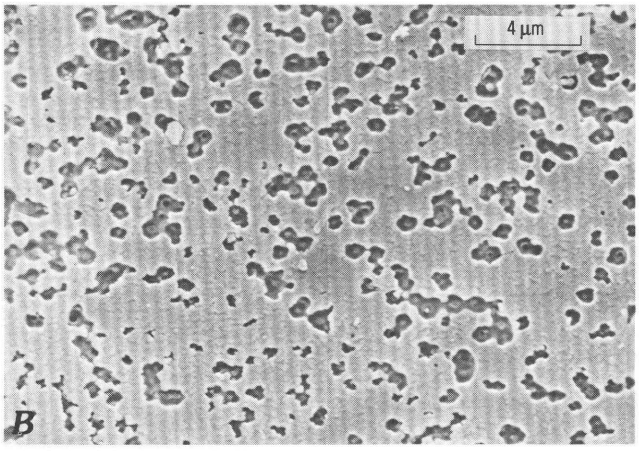

Figure 5. Scanning electron micrographs showing dissolution features of silicic, vitric shards from vitric tuffs. *A*, Corroded surface of shard. Locality 16, figure 2; sample HL–16A. *B*, Pitted shard. Locality 25, figure 2; sample HL–25–1B.

Figure 6. Ripple marks preserved in clinoptilolite-rich tuff at locality 14 (fig. 2). Pocket knife (8 cm long) shown for scale.

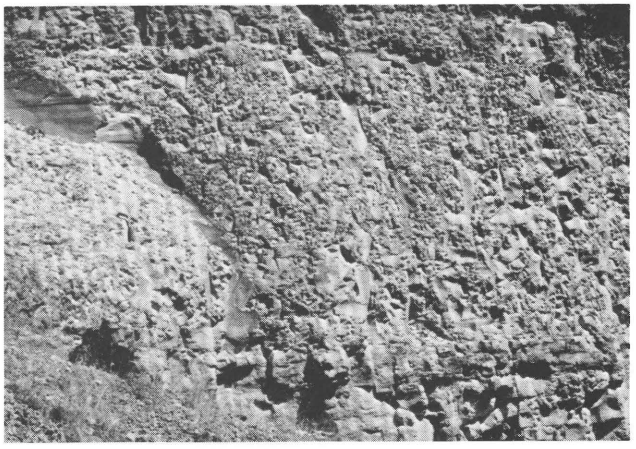

Figure 7. Zeolitic tuff that breaks with a conchoidal fracture at locality 22 (fig. 2). The tuff is green and medium to thick bedded and consists mainly of clinoptilolite and mordenite. Geologic pick (28 cm long) shown for scale in left center of photograph.

shards are hydrated. All other silicic tuffs are presumed to be rhyolitic on the basis of the low index of refraction of the glass shards and the coexisting pyrogenic minerals as described preceding.

Unlike the relatively unaltered tuff, zeolitic tuff is resistant and commonly ledge forming. The zeolitic tuff is white, light gray, yellow, orange, brown, or green, relatively hard, and dull or earthy. Original textures and sedimentary structures are generally preserved (fig. 6). The zeolitic tuff breaks with a platy, hackly, or conchoidal fracture (fig. 7).

ASH-FLOW TUFF

Walker and Swanson (1968, p. L11) recognized two ash-flow tuff units interbedded with the Miocene lacustrine rocks east of Harney Lake and correctly interpreted that both had entered a shallow lake. Although the ash-flow tuffs had not been named when Walker and Swanson investigated the geology of the area, their locality descriptions combined with observations made during the present study indicate that the tuffs are the Prater Creek and Rattlesnake Ash-flow Tuffs. Actually, throughout the present study area, the

Table 1. Chemical analyses of the unaltered basal part of the Rattlesnake Ash-flow Tuff and unaltered shards separated from vitric tuff near Harney Lake, Harney County, Oregon.
[In percent. Chemical analyses by X-ray fluorescence, H_2O determined by loss on ignition at 925°C. Analysts: D.F. Siems and J.E. Taggart]

Sample	1	2	3
SiO_2	74.2	72.1	70.6
Al_2O_3	11.5	10.6	11.1
Fe_2O_3	0.97	2.23	1.27
MgO	0.11	0.24	0.58
CaO	0.28	0.54	0.73
Na_2O	3.47	2.77	3.24
K_2O	4.86	4.68	5.51
TiO_2	0.11	0.15	0.13
P_2O_5	<0.05	<0.05	<0.05
MnO	0.07	0.03	0.07
H_2O	3.80	5.65	5.91
Total	99.37	98.99	99.14

Sample descriptions

1. Sample HL–40A; platy shards separated from vitric tuff; SE¼SW¼ sec. 26, T. 27 N., R. 30 E.
2. Sample HL–66–2; pumice shards separated from vitric tuff; SW¼NW¼ sec. 18, T. 28 S., R. 31 E.
3. Sample HL–48–13; basal unaltered, nonwelded part of Rattlesnake Ash-flow Tuff; NE¼NW¼ sec. 14, T. 28 S., R. 30 E.

Devine Canyon and Prater Creek Ash-flow Tuffs probably were deposited in the ancient lake. Only the basal part of the Rattlesnake Ash-flow Tuff, however, locally shows evidence of having been deposited in a shallow lake. All three ash-flow tuff units characteristically are welded and lack diagenetic alteration where unaffected by lacustrine deposition, but they are typically nonwelded and highly altered to zeolites where deposited in a lake.

The lacustrine facies of the Devine Canyon Ash-flow Tuff crops out only in the southern part of the study area. Exposures are generally poor, and the base was not recognized, although tuff as thick as 20 m crops out along the southern flank of Saddle Butte. The tuff is light gray where fresh but yellowish brown where weathered. Bedding is thick and indistinct; some beds show reversed graded bedding. An abundance of pyrogenic crystal fragments and large, angular pieces of pumice characterizes this tuff. The crystals make up 20–30 percent of the tuff and consist of sanidine, quartz, sodic plagioclase, green clinopyroxene, and zircon, although sanidine greatly predominates. Pumice fragments are as long as 20 cm long and are not squashed. The tuff is not welded but is cemented by authigenic zeolites, potassium feldspar, and clay minerals, although some relict glass is locally present.

The lacustrine facies of the Prater Creek Ash-flow Tuff (fig. 8) crops out in the northern and central parts of the study

Figure 8. Resistant ledge of clinoptilolite-rich Prater Creek Ash-flow Tuff at locality 4 (fig. 2). View to northwest.

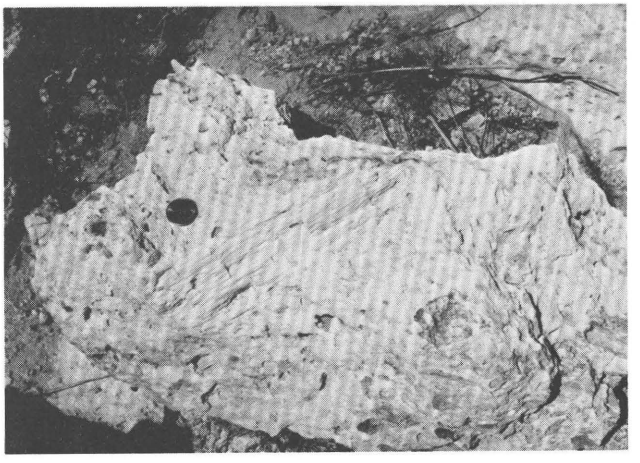

Figure 9. Closeup view of clinoptilolite-rich Prater Creek Ash-flow Tuff at locality 4 (fig. 2) showing large fragment of pumice below and to the right of coin that is 2.5 cm in diameter. Weathering of numerous smaller fragments of altered pumice from the tuff has resulted in abundant cavities.

area; the tuff is not present in the southern part of the area because of nondeposition. The tuff is light gray to yellowish gray and commonly 12–18 m thick. Bedding is thick and indistinct. Pyrogenic crystal fragments make up a percent or less of the rock and consist of quartz and sanidine. Large (as long as 22 cm) fragments of undeformed pumice are common (fig. 9). Although some relict glass is present locally, most of the originally vitric material has been altered to zeolites (Sheppard, 1993).

The Rattlesnake Ash-flow Tuff is welded, gray but reddish brown weathering, and about 12 m thick (fig. 10). Pyrogenic crystals of quartz, sanidine, plagioclase, and

Figure 10. Thick (about 75 m) sequence of yellowish-brown, tuffaceous, lacustrine rocks capped by welded Rattlesnake Ash-flow Tuff at locality 24 (fig. 2), about 0.6 km east of Harney Lake. View to east.

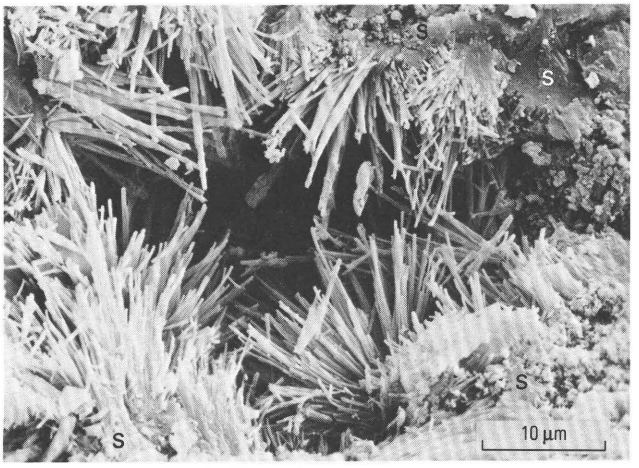

Figure 11. Scanning electron micrograph showing hollow pseudomorph of a shard consisting of acicular mordenite that grew on marginal smectite (S). Locality 49, figure 2; sample HL–49.

clinopyroxene make up a percent or less of the tuff. The originally vitric material is typically flattened and devitrified. Locally, the basal 1–9 m is nonwelded, yellow, and altered to clay minerals and zeolites where the tuff entered a shallow lake. Angular fragments of pumice in this basal nonwelded part are as long as 30 cm and undeformed.

DIAGENETIC PETROLOGY OF THE TUFFACEOUS ROCKS

The mineralogy of the altered tuffaceous rocks was determined mainly by study of X-ray diffractometer powder patterns of bulk samples (see appendix), supplemented by thin section study and scanning electron microscopy. Thin section study and scanning electron microscopy were especially useful for determining the age relationships of the authigenic minerals, but these techniques were not used until the mineralogy was determined by X-ray methods.

Although the abundance of unaltered glass in the tuffaceous sedimentary rocks increases toward the southern part of the area, tuff consisting entirely of unaltered vitric material has not been recognized. Some tuff at the southern part of the area consists of as much as 90 percent unaltered glass, but most tuff lacks glass or contains minor relict glass and variable amounts of authigenic smectite, zeolites, and opal-CT. Relict glass has been recognized as coexisting with authigenic chabazite, clinoptilolite, erionite, and phillipsite. Authigenic mordenite, analcime, and potassium feldspar also are present in some altered tuff but apparently do not coexist with vitric material. Even where no relict glass remains

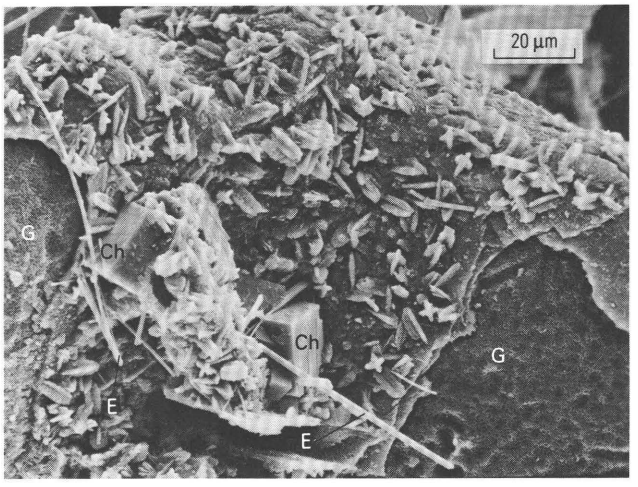

Figure 12. Scanning electron micrograph showing abundant ragged plates of minute chabazite crystals, several relatively large rhombohedra of chabazite (Ch), and fibers of erionite (E) that grew on pitted glass (G). The paragenetic sequence of zeolites, from early to late, is ragged plates of chabazite, large rhombohedra of chabazite, and then erionite. Locality 25, figure 2; sample HL–25–1B.

in the tuffaceous rocks, the vitroclastic texture is generally preserved by the authigenic minerals.

Typical pseudomorphs after bubble-wall shards consist of a thin (2–10 µm) marginal layer of smectite that is succeeded inward by crystals of one or more zeolites. The pseudomorphs may be solid or hollow, and commonly both types can be recognized in the same specimen. Hollow pseudomorphs (fig. 11) are more common than solid ones

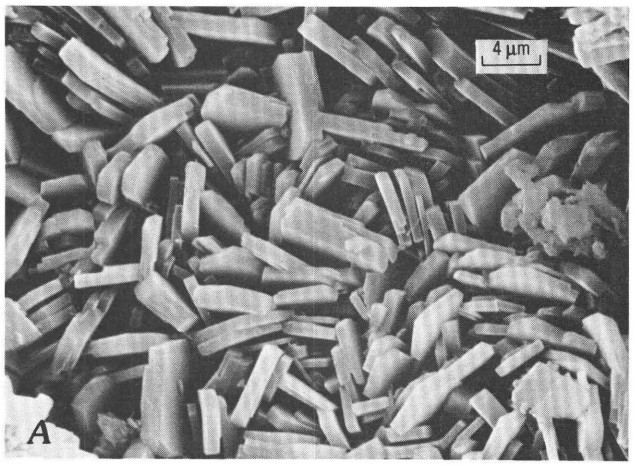

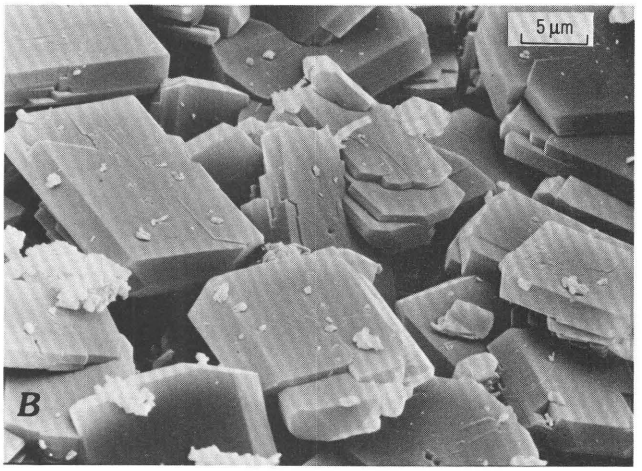

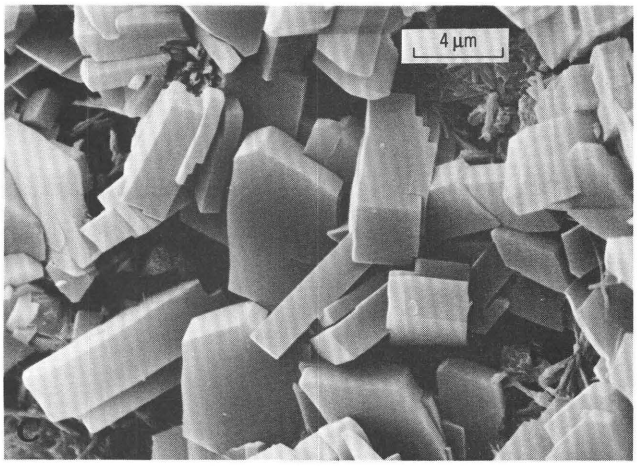

Figure 13. Scanning electron micrographs of clinoptilolite. *A*, Platy clinoptilolite. Locality 18, figure 2; sample HL–18F. *B*, Platy clinoptilolite that has well-developed crystal faces. Locality 53, figure 2; sample HL–53B. *C*, Tabular to blocky clinoptilolite. Locality 40, figure 2; sample HL–40B.

Table 2. Chemical analyses and unit-cell contents of almost monomineralic clinoptilolite-rich tuff near Harney Lake, Harney County, Oregon.

[In percent. Chemical analyses by X-ray fluorescence, H_2O determined by loss on ignition at 925°C. Analysts: D.F. Siems and J.E. Taggart]

Sample	1	2	3	4	5
SiO_2	66.8	64.8	65.1	65.0	66.4
Al_2O_3	10.7	11.6	11.1	11.7	11.3
Fe_2O_3	1.07	0.49	0.65	0.95	0.93
MgO	0.83	1.39	1.04	0.11	0.79
CaO	2.40	2.37	1.97	0.18	1.31
Na_2O	2.46	1.11	1.29	5.22	3.23
K_2O	1.42	3.08	3.20	2.12	2.19
TiO_2	0.12	0.06	0.19	0.09	0.15
P_2O_5	<0.05	<0.05	<0.05	<0.05	<0.05
MnO	0.02	<0.02	<0.02	<0.02	0.06
H_2O	13.8	15.0	13.9	14.1	13.3
Total	99.62	99.90	98.44	99.47	99.66
Atoms per unit cell (O=72)					
Si	29.87	29.47	29.76	29.52	29.71
Al	5.69	6.22	5.98	6.26	5.96
Fe^{+3}	0.36	0.17	0.22	0.32	0.31
Mg	0.55	0.94	0.71	0.07	0.53
Ca	1.15	1.16	0.96	0.09	0.63
Na	2.13	0.98	1.14	4.60	2.80
K	0.81	1.79	1.87	1.23	1.25
H_2O	20.58	22.66	21.18	21.35	19.84
$Si:(Al+Fe^{+3})$	4.94	4.61	4.80	4.49	4.74

Sample descriptions

1. Sample HL–1; thick-bedded tuff; NE¼NE¼ sec. 14, T. 27 S., R. 30 E.
2. Sample HL–4A; Prater Creek Ash-flow Tuff; SE¼NE¼ sec. 28, T. 27 S., R. 30 E.
3. Sample HL–14A; thick-bedded tuff; SE¼SW¼ sec. 26, T. 27 S., R. 30 E.
4. Sample HL–15; thick-bedded tuff; NE¼NW¼ sec. 10, T. 27 S., R. 30 E.
5. Sample HL–53B; Prater Creek Ash-flow Tuff; SE¼NW¼ sec. 13, T. 27 S., R. 30 E.

and can be recognized even with a hand lens. The larger pseudomorphs generally are hollow. Hollow pseudomorphs are convincing evidence that at least some of the zeolites crystallized in cavities from which the glass had already been dissolved.

Rarely, some zeolitic specimens seem to lack authigenic smectite, and, in others, chabazite or erionite grew directly on the relict glass shards (fig. 12).

DIAGENETIC MINERALOGY

CLINOPTILOLITE

Clinoptilolite is by far the most widespread and abundant zeolite in the altered tuffaceous rocks (see appendix)

and is present as well-formed platy, tabular, or blocky crystals that are from 2 to 70 μm long but mostly 8–30 μm long (fig. 13). The abundance of clinoptilolite in tuff ranges from trace amounts to about 100 percent but commonly is 80 percent or greater, especially at the northern part of the area. Clinoptilolite was observed to coexist with each of the other zeolites, as well as with smectite, opal-CT, and potassium feldspar.

X-ray fluorescence analyses of five almost monomineralic clinoptilolitic tuff samples (table 2) suggested that the $Si:(Al+Fe^{+3})$ ratio is about 4.5–4.9 and that the exchangeable cations are variable. Energy-dispersive X-ray analyses of clinoptilolite from other tuffs showed a range in Si:Al ratios of about 4.5–5.0. Alkalis (Na+K) exceed alkaline earths (Ca+Mg) in all the analyses.

CHABAZITE

Chabazite is present mainly at the southern part of the area where it makes up a trace to 70 percent of the tuffs. Most of the chabazite-bearing tuff contain less than 30 percent chabazite, and about half of them contain only a trace. The size and morphology of the chabazite crystals are variable. The crystal size is 0.3–50 μm, and crystals larger than about 10 μm are commonly well-formed rhombohedra that are twinned (fig. 14). Chabazite less than about 2 μm in size generally is present as a mat of malformed crystals. Aggregates of minute (less than 1 μm in size), malformed crystals also make up ragged plates (fig. 15). Locally, the large, well-formed crystals coexist with the small, malformed crystals, and the larger chabazite crystals formed later than the smaller ones (fig. 12). Chabazite was observed to coexist with all of the other zeolites except mordenite, but its coexistence with clinoptilolite or erionite is especially common. Chabazite also coexists with smectite, opal-CT, and potassium feldspar. Energy-dispersive X-ray analyses showed that the Si:Al ratio for chabazite is 3.5–4.0, consistent with derivation from a silicic glass (Gude and Sheppard, 1978).

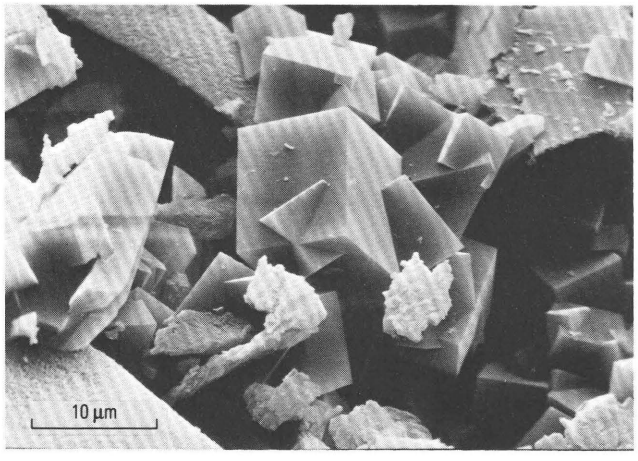

Figure 14. Scanning electron micrograph showing twinned rhombohedra of chabazite. Locality 47, figure 2; sample HL–47C.

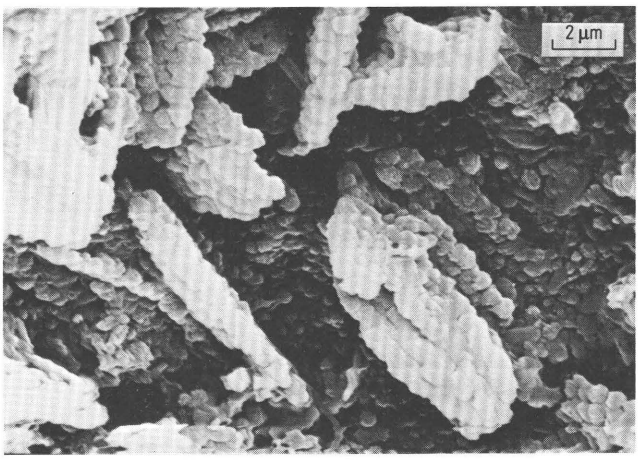

Figure 15. Scanning electron micrograph showing ragged plates that consist of aggregates of minute, malformed chabazite. Locality 25, figure 2; sample HL–25–1B.

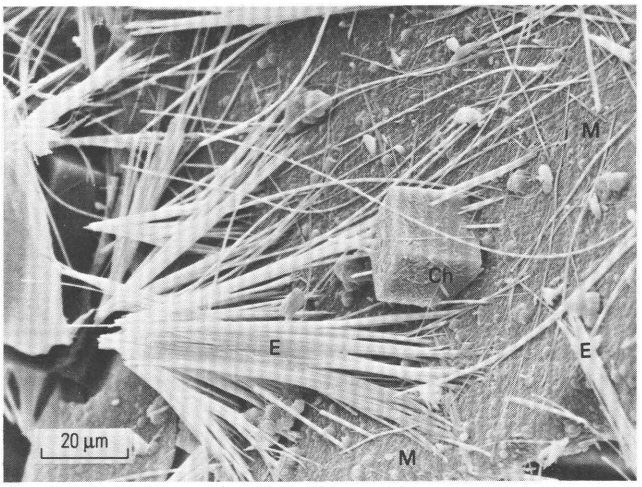

Figure 16. Scanning electron micrograph showing acicular and fibrous erionite crystals of various sizes. Erionite (E) grew on a mat (M) of minute, malformed chabazite and on a relatively large rhombohedron of chabazite (Ch), clearly indicating that it postdated both varieties of chabazite. Locality 40, figure 2; sample HL–40A.

ERIONITE

Erionite is widespread in the tuffaceous rocks near Harney Lake, but it is most common and abundant at the southern

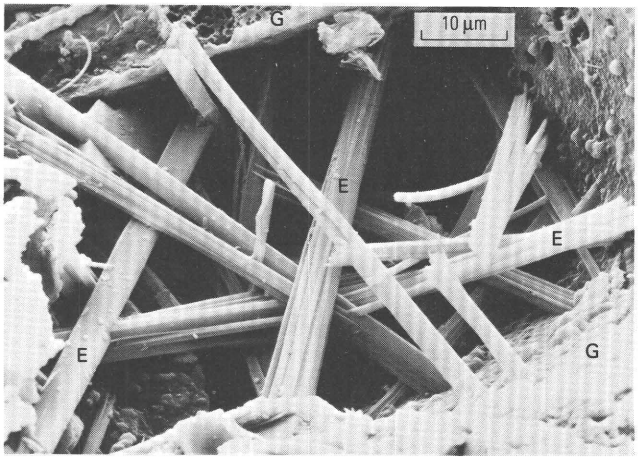

Figure 17. Scanning electron micrograph showing erionite crystals that exhibit split ends. The erionite (E) grew in a cavity among corroded glass shards (G). Locality 27, figure 2; sample HL–27.

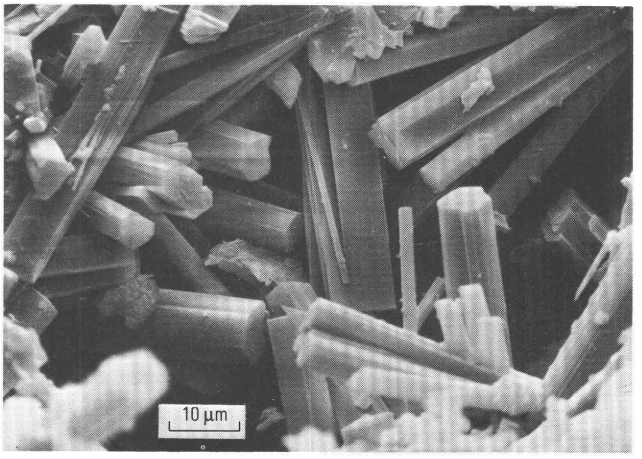

Figure 18. Scanning electron micrograph showing well-formed hexagonal prisms of erionite that are terminated by pinacoidal faces. Locality 47, figure 2; sample HL–47C.

part of the area. The erionite content ranges from a trace to about 50 percent of the tuffaceous rocks, but about 40 percent of the samples contain only a trace of this zeolite. Erionite is present as acicular, fibrous, or prismatic crystals that are 2–500 µm long (fig. 16). Most erionite, however, is less than 100 µm long. Locally, the acicular or prismatic crystals are in bundles or radial aggregates (fig. 4). More rarely, the erionite exhibits split ends (fig. 17) or well-formed hexagonal prisms (fig. 18). Erionite was observed to coexist with all of the other zeolites, as well as with authigenic smectite and opal-CT. Energy-dispersive X-ray analyses yielded Si:Al ratios of 3.6–3.7, within the range characteristic for erionite from silicic tuffs in lacustrine deposits (Gude and Sheppard, 1981).

MORDENITE

Mordenite is one of the less common zeolites in the tuffaceous rocks near Harney Lake and makes up a trace to 90 percent of the rock. About half of the samples consist of 20 percent or less mordenite, and the zeolite is most common at the northern part of the area. Mordenite is present as acicular (fig. 11) or filiform crystals that are 1–60 µm long and less than 1 µm thick. Rarely, the filiform mordenite is present as an indescribable tangle of mostly curved fibers

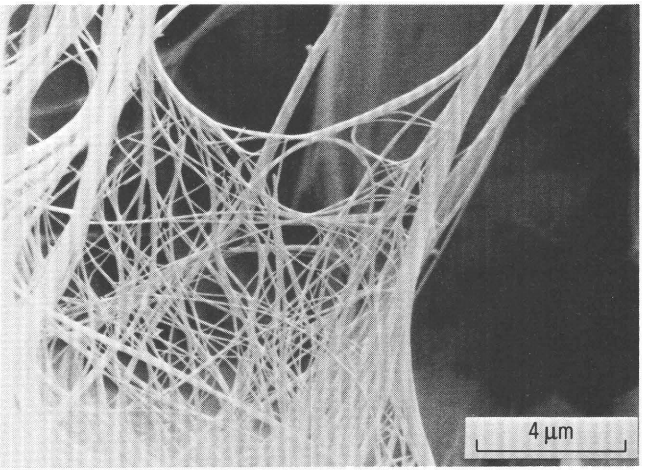

Figure 19. Scanning electron micrograph showing a tangle of curved, filiform mordenite. Locality 22, figure 2; sample HL–22–3.

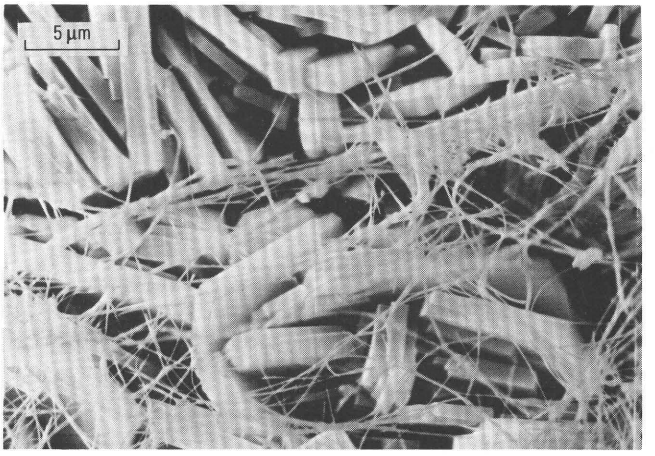

Figure 20. Scanning electron micrograph showing filiform mordenite draped across platy clinoptilolite, indicating that mordenite crystallized later than clinoptilolite. Locality 1, figure 2; sample HL-1.

Table 3. Chemical analysis and unit-cell contents of mordenite-rich tuff near Harney Lake, Harney County, Oregon.
[In percent. Chemical analysis by X-ray fluorescence, H_2O determined by loss on ignition at 925°C. Analysts: D.F. Siems and J.E. Taggart]

SiO_2	65.3
Al_2O_3	9.56
Fe_2O_3	3.46
MgO	0.62
CaO	1.55
Na_2O	2.29
K_2O	3.75
TiO_2	0.21
P_2O_5	0.06
MnO	<0.02
H_2O	11.3
Total	98.10
Atoms per unit cell (O=96)	
Si	39.52
Al	6.82
Fe^{+3}	1.58
Mg	0.56
Ca	1.00
Na	2.68
K	2.89
H_2O	22.80
$Si:(Al+Fe^{+3})$	4.70
Sample description	
Sample HL–49; nonwelded Devine Canyon Ash-flow Tuff; SE¼SE¼ sec. 36, T. 27 S., R. 30 E.	

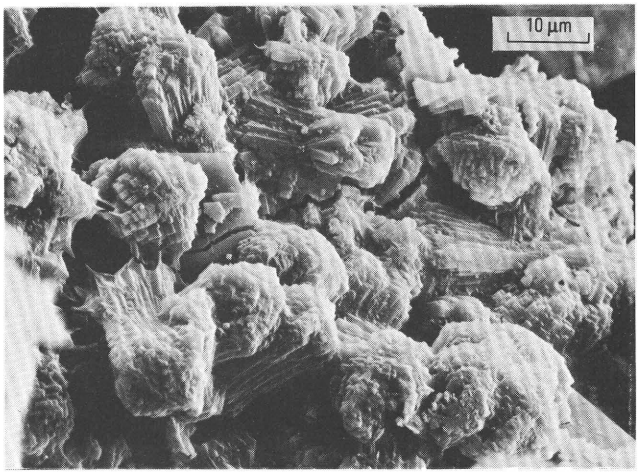

Figure 21. Scanning electron micrograph showing bundles of stubby crystals of phillipsite. Locality 25, figure 2; sample HL–25–8C.

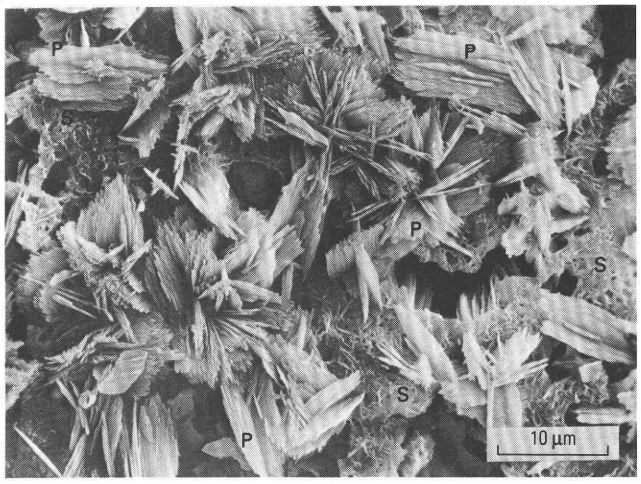

Figure 22. Scanning electron micrograph showing ragged plates of acicular phillipsite (P) that grew on smectite (S). Locality 16, figure 2; sample HL–16B.

(fig. 19). Mordenite was observed to coexist with clinoptilolite, erionite, and analcime, but its coexistence with clinoptilolite is by far the most common association. Mordenite also coexists with authigenic smectite, opal-CT, and potassium feldspar. Filiform mordenite commonly is draped across clinoptilolite crystals (fig. 20), clearly showing that the mordenite crystallized later than the clinoptilolite. The filiform mordenite generally is not recognizable in thin sections, but scanning electron microscopy is ideal for examination.

A chemical analysis by X-ray fluorescence of a mordenite-rich tuff from the Devine Canyon Ash-flow Tuff (table 3) showed that the $Si:(Al+Fe^{+3})$ ratio is 4.7 and that monovalent cations exceed divalent ones. The potassium content is particularly high (Passaglia, 1975), but it is unknown whether this high value is representative of all mordenite at Harney Lake.

PHILLIPSITE

Phillipsite is present chiefly in the southern part of the area and makes up a trace to 90 percent of the rock. More than half of the samples contain 20 percent or less phillipsite. This zeolite is present as aggregates of acicular or prismatic crystals that are 4–40 µm long; the aggregates are stubby bundles (fig. 21), ragged plates (fig. 22), or rosettes. Phillipsite was observed to coexist with all of the other zeolites except mordenite. The association of phillipsite with both clinoptilolite (fig. 23) and erionite is especially common. Phillipsite also coexists with authigenic smectite and opal-CT. Semiquantitative energy-dispersive X-ray analyses yielded Si:Al ratios of 3.2–3.5; these ratios are consistent with phillipsite that formed in silicic, vitric tuffs of other alkaline, saline-lake deposits (Sheppard and Fitzpatrick, 1989).

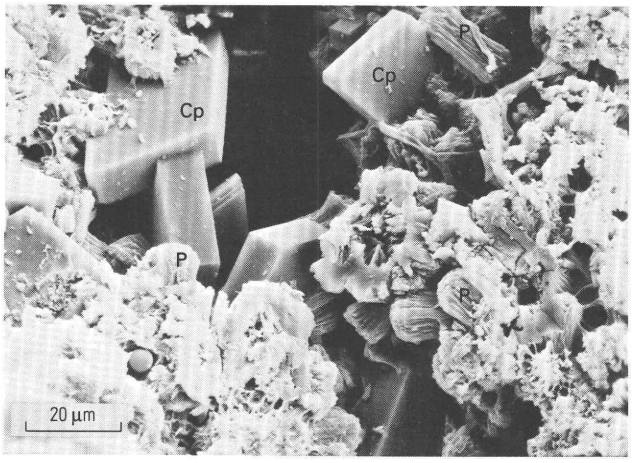

Figure 23. Scanning electron micrograph showing platy clinoptilolite (Cp) that grew in a cavity among stubby bundles of phillipsite (P). Locality 25, figure 2; sample HL–25–8C.

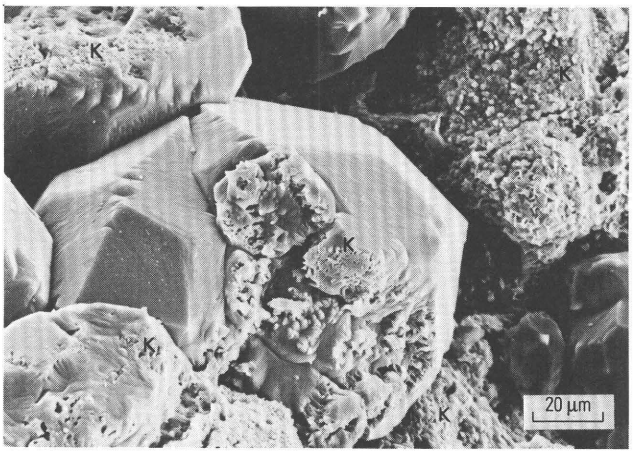

Figure 24. Scanning electron micrograph showing trapezohedra of analcime that were slightly corroded prior to partial replacement by potassium feldspar (K). Locality 24, figure 2; sample HL–24–4A.

ANALCIME

Analcime is a relatively rare zeolite in the tuffaceous rocks near Harney Lake; it is present chiefly in the central part of the area and makes up 10–70 percent of the rocks. Most samples, however, contain 20 percent or less analcime. The analcime is present as subhedral to euhedral trapezohedra that are from 20 to 300 µm in diameter, but most are less than 100 µm in diameter. Some analcime shows etched crystal faces, and some is replaced by finely crystalline potassium feldspar (fig. 24). Analcime was observed to coexist with all of the other zeolites, as well as with authigenic smectite, opal-CT, and potassium feldspar; it does not coexist with relict vitric material.

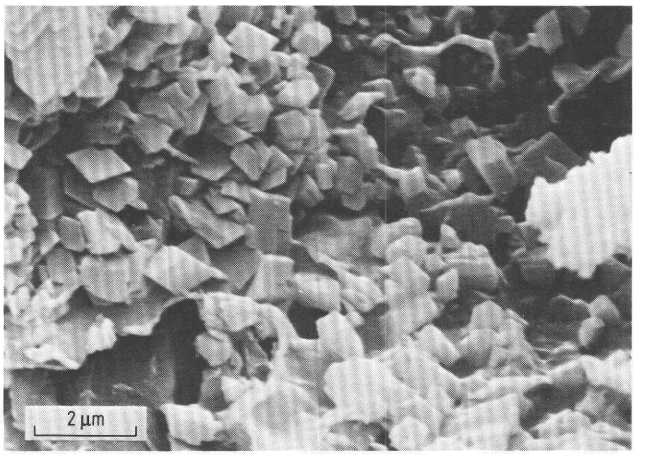

Figure 25. Scanning electron micrograph showing minute, monoclinic crystals of authigenic potassium feldspar. Locality 42, figure 2; sample HL–42.

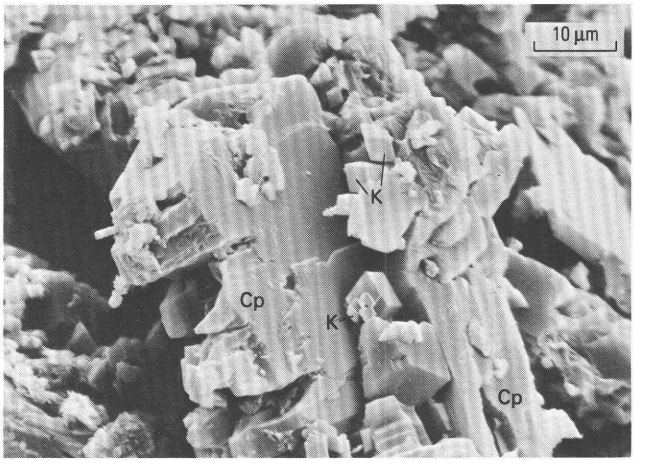

Figure 26. Scanning electron micrograph showing potassium feldspar (K) that grew on corroded clinoptilolite (Cp). Locality 69, figure 2; sample HL–69B.

POTASSIUM FELDSPAR

Authigenic potassium feldspar is present chiefly in the central part of the area and makes up a trace to about 90 percent of the rocks. The feldspar was identified on the basis of its distinctive X-ray diffractometer pattern (Sheppard and Gude, 1969) in bulk samples and its distinctive morphology as seen in scanning electron micrographs. The minute, subhedral to euhedral monoclinic crystals (fig. 25) are from 0.5 to 8 µm in size, but most are less than 4 µm in size. In those tuffaceous rocks where potassium feldspar is abundant, the vitroclastic texture commonly is vague to nonexistent. Potassium feldspar was observed to coexist with all of the zeolites except phillipsite; it may even coexist with phillipsite, but this relationship was not recognized. The potassium feldspar also coexists

Table 4. Chemical analysis of an authigenic, potassium feldspar-rich tuff, Harney County, Oregon.

[In percent. Chemical analyses by X-ray fluorescence, H_2O determined by loss on ignition at 925°C. Analysts: D.F. Siems and J.E. Taggart. A, uncorrected analysis; B, analysis corrected for CO_2 plus equivalent CaO to make calcite and then normalized to 100 percent]

	A	B
SiO_2	60.3	64.97
Al_2O_3	15.7	16.91
Fe_2O_3	1.95	2.10
MgO	0.30	0.32
CaO	3.73	0.22
Na_2O	1.14	1.23
K_2O	12.3	13.25
TiO_2	0.06	0.06
P_2O_5	<0.05	0.00
MnO	<0.02	0.00
H_2O	0.87	0.94
CO_2	2.77	0.00
Total	99.12	100.00

Sample description

Sample HL–64; thin-bedded tuff associated with Magadi-type chert; impurities include minor calcite and smectite and trace amounts of quartz, plagioclase, biotite, and hydrous iron oxide; SE¼NW¼ sec. 23, T. 27 S., R. 30 E.

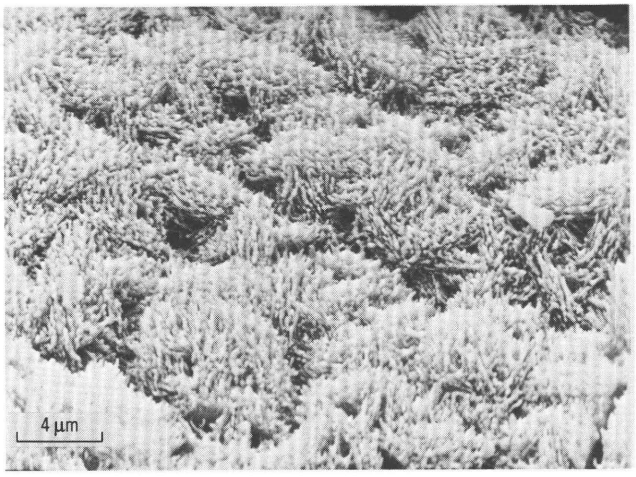

Figure 27. Scanning electron micrograph showing aggregates of ragged crystals of opal-CT. Locality 62, figure 2; sample HL–62B.

with authigenic smectite, quartz, and opal-CT, but it does not coexist with relict vitric material. The authigenic feldspar locally has replaced clinoptilolite (fig. 26), mordenite, and analcime (fig. 24), but other replacements are also probable.

A calcite-free chemical analysis by X-ray fluorescence of a tuff rich in authigenic potassium feldspar (table 4) shows a high K_2O content (13.25 percent) consistent with the high authigenic feldspar content and similar to

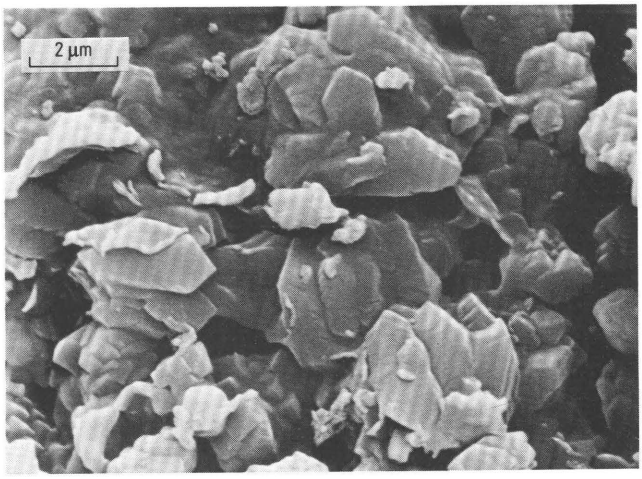

Figure 28. Scanning electron micrograph showing irregular aggregates of subhedral authigenic quartz. Locality 89, figure 2; sample HL–89B.

K_2O contents of other lacustrine tuffs that were diagenetically altered to potassium feldspar, such as those in the Miocene Barstow Formation of southern California (Sheppard and Gude, 1969).

OPAL-CT

Opal-CT is difficult to recognize in thin sections of the altered tuffaceous rocks because of its isotropic and finely crystalline character. Most identifications of opal-CT (see appendix) are based on X-ray diffractometer data or scanning electron microscopy. Where recognized, the opal makes up a trace to about 90 percent of the rock, but the content is commonly 10 percent or less. The opal-CT has relatively broad diffractometer peaks at the following d spacings: 4.29–4.33 Å, 4.06–4.11 Å, and 2.50–2.51 Å. The peak near 4.1 Å has, by far, the strongest intensity. Scanning electron micrographs show that the opal-CT is present as aggregates of elongated, ragged crystals about 1–2 mm long and less than 1 mm thick (fig. 27). Opal-CT was observed to coexist with all of the zeolites, as well as with authigenic smectite and potassium feldspar. It also rarely coexists with relict vitric material.

QUARTZ

Most of the quartz identified by X-ray diffraction of bulk samples of the tuffaceous rocks (see appendix) is epiclastic or pyrogenic. Some authigenic quartz, however, was recognized by examination of thin sections and by scanning electron microscopy. The authigenic quartz is present as irregular aggregates of minute, subhedral crystals that are

commonly 1–5 μm long (fig. 28). The relationship between quartz and the other authigenic minerals is mostly unknown, but clinoptilolite and smectite are replaced locally by quartz. Where quartz replacement has occurred, the relict vitroclastic texture is vague or absent.

SMECTITE

Smectite is an almost ubiquitous, but commonly minor, authigenic mineral in the tuffaceous rocks near Harney Lake (see appendix). It has a characteristic flaky to crenulated morphology. The first-order basal spacing is about 14.2–15.5 Å for oriented, air-dried samples and about 17.0–17.2 Å for oriented, glycolated samples. The (060) reflection is 1.49–1.50 Å and is typical for dioctahedral smectite (montmorillonite). Where it coexists with other authigenic minerals, the smectite is the earliest mineral to have crystallized.

OTHER AUTHIGENIC MINERALS

In addition to the authigenic minerals described preceding, calcite, dolomite, gypsum, fluorite, cristobalite, and halite of presumed diagenetic origin were identified in the tuffaceous rocks by X-ray diffraction of bulk samples. Except for calcite, these other constituents are rare and commonly are present in only trace amounts. For example, fluorite was identified only as a trace constituent in two samples. Calcite is present in discrete beds, commonly containing ostracodes, and as a constituent of the tuffaceous rocks in which it generally makes up a trace to 20 percent of the rock. Where recognized in thin sections of tuffaceous rocks, the calcite is present as aggregates of anhedral crystals. Calcite locally replaced pyrogenic, epiclastic, and diagenetic minerals in the tuffaceous rocks and was the latest mineral to crystallize.

PARAGENESIS

The relative age relationships of diagenetic minerals in the Miocene tuffaceous rocks near Harney Lake were determined by the sequence of filling of voids and once-hollow pseudomorphs of vitric particles and by replacement. The mineral in the interior of a void or pseudomorph presumably crystallized later than the mineral(s) nearer the periphery. The following sequences of crystallization were determined on the basis of thin section and scanning electron microscopy examination (the earliest mineral is listed first):

Smectite—clinoptilolite
Smectite—clinoptilolite—mordenite
Smectite—clinoptilolite—erionite
Smectite—clinoptilolite—analcime
Smectite—clinoptilolite—calcite
Smectite—clinoptilolite—quartz
Smectite—clinoptilolite—mordenite—erionite
Smectite—chabazite—erionite
Smectite—chabazite—clinoptilolite—erionite
Smectite—phillipsite—clinoptilolite
Smectite—phillipsite—erionite
Smectite—phillipsite—opal-CT
Smectite—phillipsite—clinoptilolite—erionite—analcime
Smectite—mordenite
Smectite—mordenite—potassium feldspar
Smectite—analcime—potassium feldspar
Clinoptilolite—potassium feldspar
Chabazite—erionite—calcite

The first three sequences are the common paragenetic sequences observed in the tuffaceous rocks. Smectite consistently crystallized prior to any of the zeolites. Phillipsite and (or) chabazite succeeded smectite and preceded clinoptilolite. Mordenite postdated clinoptilolite, and erionite postdated all of the zeolites except analcime, which was the latest zeolite to crystallize in the tuffaceous rocks. Potassium feldspar postdated analcime, as well as all of the other zeolites. Both quartz and calcite are late diagenetic minerals, and calcite probably is the latest phase because it locally shows replacement relationships with all coexisting minerals.

Some of the zeolites show dissolution effects that were recognized by scanning electron microscopy. Where

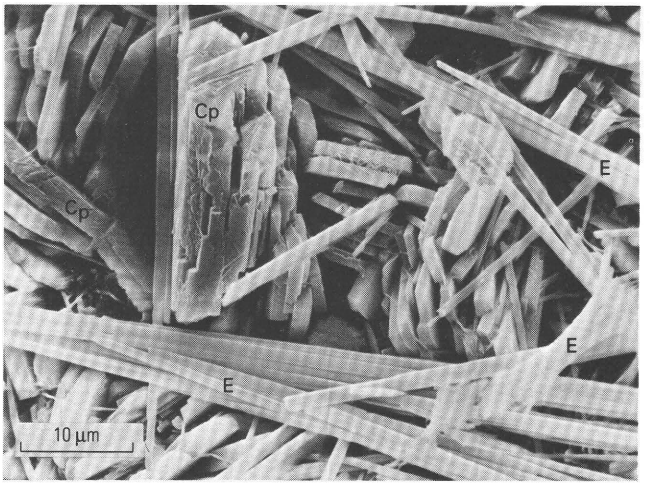

Figure 29. Scanning electron micrograph showing fibers of erionite (E) that are interstitial to or lying across clinoptilolite (Cp). The clinoptilolite was corroded prior to crystallization of minute fibers of mordenite that coat the clinoptilolite. Thus, the paragenesis of zeolites, from early to late, is clinoptilolite, mordenite, and then erionite. Locality 1, figure 2; sample HL–1.

clinoptilolite and mordenite coexist, the clinoptilolite commonly has been corroded prior to the crystallization of mordenite (fig. 29). Figure 29 also shows that erionite crystallized after the corrosion of clinoptilolite and the crystallization of mordenite. Rods and fibers of erionite also have been recognized on corroded chabazite. Authigenic potassium feldspar locally grew on corroded clinoptilolite (fig. 26) and replaced etched and corroded analcime (fig. 24).

GENESIS OF DIAGENETIC SILICATE MINERALS

Factors that may control the formation and distribution of zeolites and associated diagenetic silicate minerals in sedimentary rocks are composition, permeability, and age of the host rock and metastable crystallization, temperature, pressure, and chemistry of the pore water (Hay, 1966, 1986). Inasmuch as many of the diagenetic silicate minerals in the tuffaceous rocks near Harney Lake are present within a given tuff or within a sequence of tuffs, differences in the composition, permeability, and age of the host rock cannot explain their occurrence. The tuffaceous rocks were subjected to only shallow burial; therefore, temperature and pressure during diagenesis were relatively low. In addition, the difference, if any, in the depth of burial between relatively unaltered tuff and zeolitic or feldspathic tuff was seemingly not great enough to cause the observed distribution. The present diagenetic silicate mineralogy of the tuffaceous rocks and the pattern of distribution probably reflects differences in the chemistry of pore water during diagenesis.

Experimental work by others and theoretical considerations indicate that the activity ratio of alkali ions to hydrogen ions and the activity of silica are the major chemical parameters of the pore water that control whether clay minerals or zeolites and feldspars will crystallize under conditions approximating surface temperatures and pressures (Hemley, 1959; Garrels and Christ, 1965; Hess, 1966; Barth-Wirsching and Höller, 1989). Zeolites and feldspars are favored over clay minerals by relatively high alkali ion to hydrogen ion activity ratios and by relatively high silica activities. Such conditions in nature are especially common in the depositional environment of an alkaline, saline lake (Surdam and Sheppard, 1978).

The zeolites and associated authigenic silicate minerals in the Miocene tuffaceous rocks near Harney Lake undoubtedly formed during diagenesis by hydrolysis and dissolution of silicic glass by interstitial water. The pattern of alteration and the lateral gradation of almost unaltered (fresh) glass to an assemblage of smectite, opal-CT, zeolites, and (or) potassium feldspar strongly suggest that the interstitial water causing the alteration was the alkaline and saline water trapped in the tuffaceous rocks during lacustrine deposition and that the lake water was laterally chemically zoned, being fresh or freshest in the southern part of the area where unaltered silicic glass is most abundant.

Bedded saline minerals, the obvious evidence for an alkaline, saline depositional environment, have not been found in the Miocene tuffaceous rocks near Harney Lake. The chemistry of the lake water must be inferred from the sedimentary rocks and the fossils and diagenetic minerals contained therein. Rare casts of relatively large (as long as 1 cm), platy crystals were recognized, however, on the bottoms of certain zeolitic tuff beds. These casts probably represent an unidentified saline mineral.

Ostracodes can provide information on the chemical composition of the ancient lakes in which they lived (Forester, 1986). A coquina of the ostracode, *Limnocythere sappaensis*, was recognized in a tuffaceous mudstone that is rich in authigenic potassium feldspar at a roadcut exposure along State Route 205 (NE¼SE¼ sec. 2, T. 27 S., R. 30 E.). At this location, the associated lacustrine strata contain thin tuffs that are rich in potassium feldspar with or without zeolites. R.M. Forester (written commun., 1988) studied this occurrence of *L. sappaensis* and suggested that the original water had a pH of 9.4–11.0 and total dissolved solids of 15–100 g/L. Ostracodes also were found elsewhere in the tuffaceous lacustrine rocks where unaltered vitric material still persists, but poor preservation prevented identification of the ostracodes at any taxonomic level (R.M. Forester, written commun., 1991).

Magadi-type chert, indicative of high salinites and high pH (9–11) (Eugster, 1969; Surdam and others, 1972; Sheppard and Gude, 1986), was recognized at several locations in the tuffaceous rocks near Harney Lake. At all locations, the associated tuffs contain diagenetic potassium feldspar or zeolites or potassium feldspar and zeolites. Nowhere is the Magadi-type chert associated with unaltered (fresh) vitric material.

FORMATION OF ZEOLITES FROM SILICIC GLASS

Solution of silicic glass by the lake water trapped during deposition of the tuffaceous rocks provided the materials necessary for crystallization of zeolites. The initial alteration of rhyolitic glass in the tuffaceous rocks by hydrolysis to form the early smectite probably raised the pH, activity of SiO_2, and $(Na^+ + K^+):H^+$ activity ratio of the pore water to levels at which zeolites such as clinoptilolite, phillipsite, or chabazite crystallized. The higher pH and salinity of the pore water also caused continual and rapid dissolution of the vitric material (Mariner and Surdam, 1970). Assuming a relatively closed system during the alteration, the crystallization of smectite and zeolites resulted in an excess of SiO_2 that crystallized chiefly as opal-CT.

Experimental work by Mariner and Surdam (1970) indicates that the Si:Al ratio of zeolite is controlled by the Si:Al ratio of the solution from which the zeolite crystallized. Their experiments show that the Si:Al ratio of the solution increases as the pH decreases. Thus, relatively siliceous zeolites, such as clinoptilolite and mordenite, are

favored over aluminous zeolites, such as phillipsite and chabazite, as pH decreases. Relatively high Na:K ratios favor mordenite over clinoptilolite (Hawkins, 1981; Barth-Wirsching and Höller, 1989). During the later stages of diagenesis near Harney Lake, slight changes in the pH and cation ratios of the pore water probably were responsible for the local minor to trace amounts of erionite that crystallized after clinoptilolite.

Changes in the pH and chemical composition of the pore waters during diagenesis produced the corrosion effects observed by scanning electron microscopy. Locally, clinoptilolite and chabazite were corroded prior to crystallization of coexisting erionite, and clinoptilolite was corroded prior to crystallization of mordenite.

REACTION OF ALKALIC, SILICIC ZEOLITES TO FORM ANALCIME

Analcime in the tuffaceous rocks near Harney Lake was the last zeolite to crystallize, and ample petrographic evidence shows that it replaced smectite, clinoptilolite, erionite, and phillipsite. Although not observed, analcime also probably replaced the other zeolites. Other studies of zeolitic tuffs from alkaline, saline lacustrine deposits (Sheppard and Gude, 1973) indicate that analcime generally forms by the reaction of early formed zeolites and interstitial fluids rather than directly from the dissolution of vitric material. The analcime in the tuffaceous rocks near Harney Lake probably formed in a similar manner, and the replacement relationships described earlier support this interpretation.

Experimental work by others indicates that the reaction of an alkalic, silicic zeolite, such as clinoptilolite, to form analcime is favored by a high Na^+:H^+ ratio (Boles, 1971; Kusakabe and others, 1981), a relatively low Si:Al ratio (Senderov, 1963), and, perhaps, a relatively low activity of H_2O in the pore fluid. A slight increase in the pH of the pore water would increase the Na^+:H^+ ratio and decrease the Si:Al ratio of the pore water, and both conditions should favor the crystallization of analcime. Increased salinity may also lower the activity of H_2O sufficiently to favor the transformation of alkalic, silicic zeolites to analcime. The above arguments are based on the assumption that chemical factors alone are responsible for the formation of analcime; however, kinetic factors may be equally, or perhaps more, important. Analcime may simply form later than the other zeolites.

REACTION OF ZEOLITES TO FORM POTASSIUM FELDSPAR

Although potassium feldspar could presumably form directly from material dissolved from the silicic glass by the pore water, there is no evidence that this process was operative in the tuffaceous rocks near Harney Lake. Scanning electron micrographs (figs. 24, 26) show that potassium feldspar grew on or replaced analcime and clinoptilolite and that these zeolites had been corroded prior to the crystallization of the feldspar. Other zeolites in the tuffaceous rocks also probably served as precursors for potassium feldspar, but the textural evidence was not observed.

Kinetic factors may have been important for the zeolite to potassium feldspar reaction, but the high pH and high salinity of the pore water certainly favored the reaction (Hay and Guldman, 1987). The concentration of potassium was probably higher in the most saline part of the lake. Coupled with the high pH, the high potassium concentration would result in a relatively high K^+:H^+ ratio suitable for the crystallization of potassium feldspar. The high pH would also result in increased solubility of SiO_2 and contribute to the stabilization of potassium feldspar (Surdam and Parker, 1972). A relatively high salinity would lower the activity of H_2O and favor the formation of anhydrous potassium feldspar from hydrous zeolites, including analcime.

SUMMARY

Miocene tuffaceous rocks near Harney Lake, Oregon, are part of the now-abandoned Danforth Formation (Piper and others, 1939), which also included interstratified ash-flow tuffs and local basalt flows. These tuffaceous sedimentary rocks are chiefly lacustrine but are locally fluviatile, particularly near the southern margin of the depositional basin. Although some tuff at the southern part of the basin contains as much as 90 percent unaltered glass, most tuff lacks glass or contains minor relict glass and various amounts of authigenic smectite, zeolites, and opal-CT. Clinoptilolite is, by far, the most abundant zeolite in the tuffaceous rocks, and some clinoptilolite-rich tuff beds locally have the grade, thickness, and extent to be considered economically exploitable. Authigenic potassium feldspar apparently was the last silicate mineral to form in the tuffaceous rocks, and it replaced precursor zeolites, including analcime.

The zeolites and coexisting silicate minerals in the tuffaceous rocks near Harney Lake formed during diagenesis by dissolution of silicic glass by pore waters of various compositions. Differences in pH and salinity of the pore waters were inherited from water that was trapped in the tuffaceous rocks during deposition in an ancient lake. The pore water ranged from dilute and almost neutral in nearshore and inlet parts of the lake to saline, alkaline brine having a pH of 9 or greater in the central part of the lake. The northward and westward transition of authigenic minerals from relict glass to zeolites and then to potassium feldspar reflects this variation in the composition of the trapped lake water. Those parts of the tuffaceous rocks that still contain vitric material probably were deposited in relatively fresh water near the major inlet of the ancient lake. Farther basinward, zeolites and potassium feldspar crystallized in the tuffaceous rocks, including the interstratified ash-flow tuffs, because of the increased pH and salinity of the lake water.

REFERENCES CITED

Barth-Wirsching, Ulrike, and Höller, Helmut, 1989, Experimental studies on zeolite formation conditions: European Journal of Mineralogy, v. 1, p. 489–506.

Boles, J.R., 1971, Synthesis of analcime from natural heulandite and clinoptilolite: American Mineralogist, v. 56, p. 1724–1734.

Eugster, H.P., 1967, Hydrous sodium silicates from Lake Magadi, Kenya—Precursors of bedded chert: Science, v. 157, p. 1177–1180.

———1969, Inorganic bedded cherts from the Magadi area, Kenya: Contributions to Mineralogy and Petrology, v. 22, p. 1–31.

Forester, R.M., 1986, Determination of the dissolved anion composition of ancient lakes from fossil ostracodes: Geology, v. 14, p. 796–798.

Garrels, R.M., and Christ, C.L., 1965, Solutions, minerals, and equilibria: New York, Harper and Row, 450 p.

Greene, R.C., 1973, Petrology of the welded tuff of Devine Canyon, southeast Oregon: U.S. Geological Survey Professional Paper 797, 26 p.

Greene, R.C., Walker, G.W., and Corcoran, R.E., 1972, Geologic map of the Burns quadrangle, Oregon: U.S. Geological Survey Miscellaneous Geologic Investigations Map I–680, scale 1:250,000.

Gude, A.J., 3d, and Sheppard, R.A., 1978, Chabazite in siliceous tuffs of a Pliocene lacustrine deposit near Durkee, Baker County, Oregon: U.S. Geological Survey Journal of Research, v. 6, p. 467–472.

———1981, Woolly erionite from the Reese River zeolite deposit, Lander County, Nevada, and its relationship to other erionites: Clays and Clay Minerals, v. 29, p. 378–384.

Hawkins, D.B., 1981, Kinetics of glass dissolution and zeolite formation under hydrothermal conditions: Clays and Clay Minerals, v. 29, p. 331–340.

Hay, R.L., 1966, Zeolites and zeolitic reactions in sedimentary rocks: Geological Society of America Special Paper 85, 130 p.

———1986, Geologic occurrence of zeolites and some associated minerals, *in* Murakami, Y., Iijima, A., and Ward, J.W., eds., New developments in zeolite science and technology: International Zeolite Conference, 7th, Tokyo, Kodonsha, August 1986, Proceedings, p. 35–40.

Hay, R.L., and Guldman, S.G., 1987, Diagenetic alteration of silicic ash in Searles Lake, California: Clays and Clay Minerals, v. 35, p. 449–457.

Heaney, P.J., Sheppard, R.A., and Post, J.E., 1992, Association of length-slow silica with evaporites: Geological Society of America Abstracts with Programs, v. 24, no. 7, p. A231.

Hemley, J.J., 1959, Some mineralogical equilibria in system K_2O-Al_2O_3-SiO_2-H_2O: American Journal of Science, v. 257, p. 241–270.

Hess, P.C., 1966, Phase equilibria of some minerals in the K_2O-Na_2O-Al_2O_3-SiO_2-H_2O system at 25°C and 1 atmosphere: American Journal of Science, v. 264, p. 289–309.

Holmes, D.A., 1990, Pacific Northwest zeolite update, *in* Geitgey, R.P., and Vogt, B.V., eds., Industrial rocks and minerals of the Pacific Northwest: Oregon Department of Geology and Mineral Industries Special Paper 23, p. 79–88.

Kusakabe, Hirotatsu, Minato, Hideo, Utada, Minoru, and Yamanaka, Takamitsu, 1981, Phase relations of clinoptilolite, mordenite, analcime and albite with increasing pH, sodium ion concentration and temperature: University of Tokyo Scientific Papers of the College of General Education, v. 31, no. 1, p. 39–59.

Mariner, R.H., and Surdam, R.C., 1970, Alkalinity and formation of zeolites in saline alkaline lakes: Science, v. 170, p. 977–980.

Mumpton, F.A., 1984, Zeolite exploration—The early days, *in* Olson, D., and Bisio, A., eds., Proceedings of the 6th International Zeolite Conference, Reno, 1983: Guildford, United Kingdom, Butterworths, p. 68–86.

Parker, D.J., 1974, Petrology of selected volcanic rocks of the Harney Basin, Oregon: Corvallis, Oregon State University, Ph.D. dissertation, 119 p.

Passaglia, Elio, 1975, The crystal chemistry of mordenites: Contributions to Mineralogy and Petrology, v. 50, p. 65–77.

Piper, A.M., Robinson, T.W., and Park, C.F., Jr., 1939, Geology and ground-water resources of the Harney Basin, Oregon: U.S. Geological Survey Water-Supply Paper 841, 189 p.

Russell, I.C., 1884, A geological reconnaissance in southern Oregon: U.S. Geological Survey Annual Report 4, p. 431–464.

Senderov, E.E., 1963, Crystallization of mordenite under hydrothermal conditions: Geochemistry, no. 9, p. 848–859.

Sheppard, R.A., 1993, Geology and mineralogy of the Harney Lake zeolite deposit, Harney County, Oregon, *in* Zeo-Trip '93, an excursion to selected zeolite and clay deposits in southeastern Oregon and southwestern Idaho, June 26–28, 1993: Brockport, New York, International Committee on Natural Zeolites, p. 42–58.

Sheppard, R.A., and Fitzpatrick, J.J., 1989, Phillipsite from silicic tuffs in saline, alkaline-lake deposits: Clays and Clay Minerals, v. 37, p. 243–247.

Sheppard, R.A., and Gude, A. J., 3d, 1968, Distribution and genesis of authigenic silicate minerals in tuffs of Pleistocene Lake Tecopa, Inyo County, California: U.S. Geological Survey Professional Paper 597, 38 p.

———1969, Diagenesis of tuffs in the Barstow Formation, Mud Hills, San Bernardino County, California: U.S. Geological Survey Professional Paper 934, 35 p.

———1973, Zeolites and associated authigenic silicate minerals in tuffaceous rocks of the Big Sandy Formation, Mohave County, Arizona: U.S. Geological Survey Professional Paper 830, 36 p.

———1986, Magadi-type chert—A distinctive diagenetic variety from lacustrine deposits, *in* Mumpton, F.A., ed., Studies in diagenesis: U.S. Geological Survey Bulletin 1578, p. 335–345.

Surdam, R.C., Eugster, H.P., and Mariner, R.H., 1972, Magadi-type chert in Jurassic and Eocene to Pleistocene rocks, Wyoming: Geological Society of America Bulletin, v. 83, p. 2261–2266.

Surdam, R.C., and Parker, R.D., 1972, Authigenic aluminosilicate minerals in the tuffaceous rocks of the Green River Formation, Wyoming: Geological Society of America Bulletin, v. 83, p. 689–700.

Surdam, R.C., and Sheppard, R.A., 1978, Zeolites in saline, alkaline-lake deposits, *in* Sand, L.B., and Mumpton, F.A., eds., Natural zeolites—Occurrence, properties, use: Elmsford, N.Y., Pergamon Press, p. 145–174.

Walker, G.W., 1979, Revisions to the Cenozoic stratigraphy of Harney Basin, southeastern Oregon: U.S. Geological Survey Bulletin 1475, 35 p.

Walker, G.W., and Nolf, B., 1981, High Lava Plains, Brothers fault zone to Harney Basin, Oregon, *in* Johnston, D.A., and Donnelly-Nolan, Julie, eds., Guides to some volcanic terranes in Washington, Idaho, Oregon, and northern California: U.S. Geological Survey Circular 838, p. 105–118.

Walker, G.W., and Swanson, D.A., 1968, Summary report on the geology and mineral resources of the Harney Lake and Malheur Lake areas of the Malheur National Wildlife Refuge, north-central Harney County, Oregon: U.S. Geological Survey Bulletin 1260–L, p. L1–L17.

APPENDIX

Appendix. Mineralogic composition of Miocene tuffaceous rocks near Harney Lake, Harney County, Oregon, as estimated from X-ray diffractometer patterns of bulk samples.
[Samples shown by locality numbers in figure 2. Sample location column shows position of sample in meters above base of outcrop at sample site; if no position is given, samples are listed from bottom to top; Tdc, Devine Canyon Ash-flow Tuff; Tpc, Prater Creek Ash-flow Tuff; Trs, Rattlesnake Ash-flow Tuff; L, below Prater Creek Ash-flow Tuff but exact stratigraphic position unknown; U, above Prater Creek Ash-flow Tuff but exact stratigraphic position unknown; Uk, stratigraphic position unknown; Ct, chert; Ls, limestone; Ms, mudstone; Ss, sandstone; St, siltstone; T, tuff. X-ray analysis results given in parts of 10. Leaders (--), looked for but not found; Tr, trace. Mica includes pyrogenic biotite and detrital muscovite and biotite. Quartz includes pyrogenic, detrital, and authigenic varieties. Alkali feldspar includes pyrogenic and detrital sodic plagioclase, sanidine, and anorthoclase. Other is chiefly hornblende; samples HL–9F and HL–26C contain a trace of fluorite; samples HL–17B and HL–45D contain 2 parts cristobalite; sample HL–24–3 contains 6 parts dolomite; sample HL–66–11B contains 1 part dolomite; sample HL–24–4A contains a trace of halite]

Locality No.	Sample No.	Sample location	Glass	Opal-CT	Mica	Smectite	Phil-lipsite	Chabazite	Erionite	Clinop-tilolite	Mordenite	Analcime	Potassium feldspar	Alkali feldspar	Quartz	Calcite	Other
1	HL–1	1.00, U, T	--	--	--	Tr	--	--	--	9	1	--	--	Tr	--	--	--
2	HL–2A	U, T	--	--	--	--	--	--	--	9	1	--	--	Tr	--	--	--
	HL–2B	U, T	--	--	--	Tr	--	--	Tr	10	--	--	--	--	--	--	--
3	HL–3	U, T	--	--	--	--	--	--	--	Tr	--	--	5	--	5	--	--
4	HL–4A	Tpc	--	--	--	Tr	--	--	--	10	--	--	--	--	--	--	--
	HL–4B	Tpc	--	--	--	Tr	--	--	--	9	--	--	--	1	--	--	--
5	HL–5A	U, T	--	--	--	--	--	Tr	--	9	--	--	--	--	--	--	--
	HL–5B	U, T	--	--	--	--	--	--	--	9	1	--	--	--	--	--	--
6	HL–6A	U, T	--	--	--	--	--	--	1	9	--	--	--	--	--	--	--
	HL–6B	U, T	--	--	--	Tr	Tr	--	--	10	--	--	--	--	--	--	--
7	HL–7	Uk, T	--	--	--	Tr	--	--	--	9	1	--	--	--	--	--	--
9	HL–9D	1.00, U, T	--	--	--	Tr	--	Tr	--	--	--	--	9	1	--	--	--
	HL–9E	1.05, U, T	--	--	--	2	--	--	--	--	--	--	8	--	--	--	--
	HL–9F	2.10, U, Ls	--	--	--	5	--	--	--	--	--	--	Tr	--	--	5	Tr
	HL–9G	2.50, U, Ct	--	--	--	2	--	--	--	--	--	--	--	--	8	--	--
	HL–9A	3.15, U, T	--	--	--	--	--	Tr	--	4	--	--	5	1	--	--	--
	HL–9B	3.40, U, Ms	--	--	--	4	--	--	--	--	--	--	5	--	--	1	--
	HL–9C	4.40, U, Ct	--	--	--	--	--	--	--	--	--	--	--	--	10	--	--
10	HL–10A	U, Ss	4	1	--	2	--	--	1	--	--	--	--	1	1	--	--
	HL–10B	U, St	2	--	1	6	--	--	Tr	--	--	--	--	1	--	Tr	--
	HL–10C	U, T	--	--	--	2	--	--	4	4	--	--	--	--	--	--	--
	HL–10D	U, T	--	--	--	1	--	--	4	5	--	--	--	--	--	--	--
11	HL–11A	U, T	--	--	--	--	--	Tr	--	2	--	--	8	--	--	--	--
	HL–11B	U, T	--	--	--	1	--	--	--	7	--	--	2	--	--	--	--
	HL–11C	U, Ct	--	--	--	--	--	--	--	--	--	--	--	--	10	Tr	--
12	HL–12	U, T	--	--	--	1	--	--	--	9	--	--	--	--	--	--	--
13	HL–13	U, T	--	--	--	1	--	--	Tr	9	--	--	--	--	--	--	--

Locality No.	Sample No.	Sample location	Glass	Opal-CT	Mica	Smectite	Phil-lipsite	Chabazite	Erionite	Clinop-tilolite	Mordenite	Analcime	Potassium feldspar	Alkali feldspar	Quartz	Calcite	Other
14	HL–14A	U, T	--	Tr	--	--	--	--	--	10	--	--	--	--	--	--	--
	HL–14B	U, T	--	1	--	--	--	--	--	9	--	--	--	--	--	--	--
15	HL–15	U, T	--	--	--	--	--	--	Tr	10	--	--	--	--	--	--	--
16	HL–16A	Trs	4	--	--	3	--	--	1	--	--	--	--	1	1	--	--
	HL–16B	Trs	5	1	--	1	3	--	--	--	--	--	--	--	--	--	--
17	HL–17A	U, Ss	--	--	--	3	--	--	2	Tr	--	--	--	5	--	--	--
	HL–17B	U, Ss	--	--	--	Tr	1	--	1	1	--	--	--	5	--	--	2
18	HL–18D	0.06, U, T	--	--	--	Tr	--	--	--	7	3	--	--	--	--	--	--
	HL–18E	1.60, U, T	--	--	--	Tr	--	--	--	8	2	--	--	--	--	--	--
	HL–18F	3.30, U, T	--	--	--	Tr	--	--	--	7	3	--	--	--	--	--	--
	HL–18G	5.70, U, T	--	--	--	--	--	--	--	8	2	--	--	--	--	--	--
	HL–18H	U, T	--	--	--	Tr	--	--	Tr	9	1	--	--	--	--	--	--
	HL–18C	U, T	--	--	--	--	--	--	--	9	--	--	--	1	--	--	--
19	HL–19	U, T	--	--	--	2	--	--	--	8	--	--	--	--	--	--	--
21	HL–21	U, T	--	1	--	Tr	--	--	--	6	2	--	--	1	--	--	--
22	HL–22–2A	0.10, U, T	--	2	--	2	--	--	--	6	--	--	--	--	--	--	--
	HL–22–2B	4.00, U, T	--	1	--	Tr	--	--	--	8	1	--	--	Tr	--	--	--
	HL–22–3	8.10, U, T	--	--	--	--	--	--	Tr	6	4	--	--	--	--	--	--
	HL–22–4	10.70, U, T	--	--	--	--	--	--	Tr	4	5	--	--	1	--	--	--
23	HL–23	U, T	5	--	--	--	--	4	--	1	--	--	--	Tr	--	--	--
24	HL–24–1A	1.00, Uk, St	--	--	--	3	--	--	--	2	--	2	2	1	--	--	--
	HL–24–1B	2.00, Uk, Ss	--	--	--	1	--	--	1	4	--	--	--	4	--	--	--
	HL–24–2A	7.70, Uk, T	--	--	--	2	--	--	--	--	--	--	8	--	--	--	--
	HL–24–2B	8.05, Uk, T	--	--	--	1	--	--	--	Tr	--	--	3	--	--	6	--
	HL–24–3	8.27, Uk, Ls	--	--	Tr	--	--	--	--	--	--	--	3	--	Tr	1	6
	HL–24–4A	13.68, Uk, St	--	--	--	3	--	--	--	--	--	2	4	1	--	--	Tr
	HL–24–4B	14.03, Uk, T	--	--	--	1	--	--	--	--	--	--	9	--	--	--	--
	HL–24–5	19.87, Uk, T	--	--	--	1	--	--	--	--	--	--	8	1	--	--	--
	HL–24–6	27.92, Uk, St	--	--	Tr	1	--	--	--	--	--	--	7	1	1	--	--
	HL–24–7	33.22, Uk, T	--	--	Tr	1	--	--	--	--	--	--	7	--	2	--	--
	HL–24–8A	41.02, Uk, T	--	--	--	1	--	--	--	--	--	--	6	--	2	1	--
	HL–24–8B	43.52, Uk, Ss	--	--	--	2	--	Tr	--	3	--	--	2	1	--	2	--
	HL–24–10	51.37, Uk, Ls	--	--	--	1	--	--	--	--	--	--	2	--	3	4	Tr
	HL–24–11	62.67, Uk, Ss	--	--	1	1	--	--	--	5	--	--	--	3	--	--	--
	HL–24–12	72.67, Uk, T	--	--	--	1	--	--	--	9	--	--	--	--	--	--	--
	HL–24–13	73.72, Uk, T	--	--	--	1	--	--	--	9	--	--	--	Tr	--	--	--
	HL–24–14A	74.00,Trs	--	--	--	1	--	--	--	--	--	--	--	6	3	--	--
	HL–24–14B	76.00,Trs	--	--	--	--	--	--	--	--	--	--	--	4	6	--	--

Appendix. Mineralogic composition of Miocene tuffaceous rocks near Harney Lake, Harney County, Oregon, as estimated from X-ray diffractometer patterns of bulk samples—Continued.

Locality No.	Sample No.	Sample location	Glass	Opal-CT	Mica	Smectite	Phillipsite	Chabazite	Erionite	Clinoptilolite	Mordenite	Analcime	Potassium feldspar	Alkali feldspar	Quartz	Calcite	Other
25	HL–25–1A	1.00, Tpc	--	1	--	--	--	5	Tr	4	--	--	--	--	--	--	--
	HL–25–1B	9.50, Tpc	6	--	--	--	--	4	--	--	--	--	--	Tr	--	Tr	--
	HL–25–3	25.20, U, T	--	8	--	--	--	--	--	2	--	--	--	--	--	--	--
	HL–25–5	31.55, U, Ss	--	--	--	1	--	--	1	4	--	--	--	4	--	--	--
	HL–25–6	34.25, U, St	--	--	Tr	5	--	--	--	2	--	--	--	--	--	3	--
	HL–25–7	34.32, U, Ls	--	--	--	4	Tr	Tr	--	3	--	--	--	--	--	3	--
	HL–25–8A	34.85, U, T	9	--	--	--	--	--	--	1	--	--	--	--	--	--	--
	HL–25–8B	35.95, U, Ls	--	--	--	1	--	--	--	1	--	--	--	--	--	8	--
	HL–25–8C	39.05, U, T	--	--	--	--	6	--	--	4	--	--	--	Tr	--	--	--
	HL–25–9A	46.20, U, T	--	--	--	1	4	--	--	5	--	--	--	--	--	--	--
	HL–25–9B	52.10, U, T	--	1	--	1	--	--	Tr	8	--	--	--	--	--	--	--
26	HL–26C	U, Ls	--	--	--	1	--	--	--	1	--	--	--	--	--	8	Tr
	HL–26A	U, Ss	--	--	1	3	--	--	1	--	--	--	--	5	Tr	--	Tr
	HL–26B	U, T	--	--	--	3	1	Tr	2	--	--	--	--	4	--	--	--
27	HL–27	Tdc	3	--	--	--	--	5	Tr	--	--	--	--	1	1	--	--
28	HL–28A	U, T	6	--	--	2	--	Tr	1	--	--	--	--	1	--	--	--
	HL–28B	U, T	4	--	--	2	1	--	2	--	--	--	--	1	--	--	--
31	HL–31A	U, T	--	1	--	1	--	--	--	8	--	--	--	--	Tr	--	--
	HL–31B	U, T	--	3	--	--	--	--	Tr	7	--	--	--	--	--	--	--
32	HL–32A	Tpc	--	--	--	Tr	--	--	--	10	--	--	--	--	--	--	--
	HL–32B	U, T	--	4	--	Tr	--	--	--	6	--	--	--	--	--	--	--
33	HL–33	U, T	--	1	--	--	--	--	Tr	6	2	1	--	--	--	--	--
34	HL–34	Tpc	--	1	--	--	--	--	Tr	9	--	--	--	--	--	--	--
36	HL–36	Tpc	--	2	--	--	--	--	Tr	8	--	--	--	--	--	--	--
37	HL–37	Tpc	--	--	--	--	--	--	Tr	10	--	--	--	--	--	--	--
38	HL–38	U, T	--	1	--	1	--	--	Tr	8	--	--	--	--	--	--	--
39	HL–39–1A	0.10, Tpc	--	--	--	--	--	--	Tr	10	--	--	--	--	--	--	--
	HL–39–1B	6.00, Tpc	--	1	--	--	--	--	Tr	9	--	--	--	--	--	--	--
	HL–39–2A	7.00, U, T	--	--	--	--	--	--	Tr	8	1	--	--	--	1	--	--
	HL–39–2B	9.20, U, T	--	--	--	--	--	--	Tr	7	2	--	--	--	1	--	--
	HL–39–3A	10.20, U, T	--	1	--	Tr	--	--	--	6	--	--	--	--	3	--	--
	HL–39–3B	13.20, U, T	--	2	--	--	--	--	--	7	1	--	--	--	--	--	--
	HL–39–3C	19.70, U, T	--	2	--	1	--	--	--	6	--	--	--	1	--	--	--
	HL–39–4A	24.55, U, T	--	--	--	2	--	--	--	6	2	--	--	--	--	Tr	--

Locality No.	Sample No.	Sample location	Glass	Opal-CT	Mica	Smectite	Phil-lipsite	Chabazite	Erionite	Clinop-tilolite	Mordenite	Analcime	Potassium feldspar	Alkali feldspar	Quartz	Calcite	Other
39	HL–39–4B	31.45, U, T	--	Tr	--	2	--	--	--	7	--	--	--	--	--	1	Tr
	HL–39–4C	36.45, U, T	--	Tr	--	2	--	--	Tr	6	--	--	--	--	--	2	--
	HL–39–4D	44.95, U, T	--	1	--	2	--	--	Tr	7	Tr	--	--	--	--	--	--
40	HL–40A	U, T	8	--	--	--	--	2	Tr	--	--	--	--	Tr	--	--	--
	HL–40B	U, T	--	--	--	Tr	--	7	--	3	--	--	--	--	--	--	--
41	HL–41	Uk, T	--	--	--	1	--	--	--	9	--	--	--	--	Tr	--	--
42	HL–42	U, T	--	--	--	1	--	--	--	Tr	--	1	8	--	--	--	--
43	HL–43A	Uk, Ms	--	--	--	6	--	--	--	--	--	2	2	--	--	--	--
	HL–43B	Uk, T	--	--	--	--	--	--	--	7	--	--	1	--	--	2	--
44	HL–44	Tdc	--	2	--	--	--	Tr	--	3	--	--	--	3	2	--	--
45	HL–45A	U, T	7	--	--	1	--	--	1	Tr	--	--	--	1	--	--	--
	HL–45B	Trs	7	--	--	--	Tr	--	3	--	--	--	--	--	--	--	--
	HL–45C	Trs	--	--	--	--	--	--	Tr	10	--	--	--	--	--	--	--
	HL–45D	Trs	--	--	--	--	--	--	--	--	--	--	--	5	3	--	2
46	HL–46A	Uk, T	8	1	--	--	--	--	Tr	1	--	--	--	--	--	--	--
	HL–46B	Uk, T	--	9	--	--	--	--	--	1	--	--	--	--	--	Tr	--
47	HL–47A	0.20, Tdc	--	--	--	3	--	--	1	--	--	--	--	5	1	--	--
	HL–47B	18.50, Uk, Ss	1	--	--	2	2	--	3	--	--	--	--	2	--	--	--
	HL–47C	23.50, Uk, Ss	--	--	--	1	2	3	3	--	--	--	--	1	--	--	--
	HL–47D	40.00, Uk, T	5	--	--	2	--	Tr	1	--	--	--	--	2	--	--	--
48	HL–48–1A	3.40, Uk, St	--	1	--	2	2	Tr	--	--	--	--	--	4	--	--	--
	HL–48–1B	4.80, Uk, Ss	--	--	--	Tr	--	--	3	3	--	--	--	4	--	--	--
	HL–48–1C	5.20, Uk, T	--	--	--	--	--	--	4	5	--	--	--	1	--	--	--
	HL–48–2	17.70, Uk, Ss	--	--	--	1	--	Tr	4	--	--	--	--	5	--	--	--
	HL–48–3	19.30, Uk, Ss	--	--	--	--	--	--	3	5	--	--	--	2	--	--	--
	HL–48–4	25.20, Uk, Ss	--	--	--	3	--	--	Tr	--	--	--	--	7	--	--	Tr
	HL–48–5	29.85, Uk, Ss	--	--	--	2	--	--	1	3	--	--	--	4	--	--	--
	HL–48–6A	32.90, Uk, Ss	--	--	--	2	--	--	Tr	3	--	--	--	5	--	--	--
	HL–48–6B	34.70, Uk, Ls	--	--	--	2	--	Tr	--	Tr	--	--	--	1	--	7	--
	HL–48–7	42.00, Uk, Ss	--	--	--	2	--	--	2	--	--	--	--	--	1	5	--
	HL–48–8	44.40, Uk, T	--	--	--	--	--	--	--	9	--	--	--	1	--	--	--
	HL–48–9	51.90, Uk, Ss	--	--	--	3	--	--	4	--	--	--	--	3	--	--	--
	HL–48–10	52.80, Uk, Ls	--	--	--	1	--	--	--	--	--	--	--	--	--	9	--
	HL–48–12	88.60, Uk, T	7	--	--	2	Tr	--	Tr	--	--	--	--	Tr	1	--	--
	HL–48–13	100.60,Trs	10	--	--	--	--	--	--	--	--	--	--	--	--	Tr	--
49	HL–49	Tdc	--	1	--	1	--	--	--	--	8	--	--	Tr	--	--	--

Appendix. Mineralogic composition of Miocene tuffaceous rocks near Harney Lake, Harney County, Oregon, as estimated from X-ray diffractometer patterns of bulk samples—Continued.

Locality No.	Sample No.	Sample location	Glass	Opal-CT	Mica	Smectite	Phil-lipsite	Chabazite	Erionite	Clinop-tilolite	Mordenite	Analcime	Potassium feldspar	Alkali feldspar	Quartz	Calcite	Other
50	HL–50A	Uk, Ss	--	--	--	3	--	--	2	2	--	--	--	3	--	--	--
	HL–50B	Uk, T	--	--	--	2	--	--	--	1	--	--	--	--	7	--	--
	HL–50C	Uk, Ct	--	--	--	--	--	--	--	--	--	--	--	--	10	--	--
51	HL–51	Uk, T	--	--	--	--	--	--	5	4	--	--	--	--	--	1	--
53	HL–53B	Tpc	--	--	--	--	--	--	Tr	10	--	--	--	--	--	--	--
	HL–53C	Tpc	--	--	--	1	--	--	--	9	--	--	--	--	--	--	--
54	HL–54A	U, T	--	--	--	--	--	--	4	5	--	--	--	1	--	--	--
	HL–54B	U, T	--	--	--	1	--	--	1	8	--	--	--	--	--	--	--
55	HL–55A	U, T	8	--	--	--	--	--	2	--	--	--	--	--	--	--	--
	HL–55B	U, T	--	--	--	--	--	--	Tr	10	--	--	--	--	--	--	--
56	HL–56	U, Ss	--	--	--	2	--	--	5	--	--	--	--	3	--	--	Tr
58	HL–58	Uk, T	--	--	--	2	--	--	2	1	--	--	--	5	--	--	--
61	HL–61	U, T	--	--	--	1	--	--	--	9	--	--	--	--	--	--	--
62	HL–62A	U, T	--	--	--	1	--	--	Tr	9	--	--	--	--	--	--	--
	HL–62B	U, T	--	6	--	--	--	--	--	3	--	--	--	1	--	--	--
63	HL–63	U, T	--	--	--	Tr	--	--	1	5	--	--	--	4	--	--	--
64	HL–64	U, T	--	--	--	Tr	--	--	--	--	--	--	9	--	--	1	--
65	HL–65	U, T	--	--	--	--	--	--	--	6	3	--	--	--	1	--	--
66	HL–66–1	19.80, Tdc	--	--	--	--	--	1	1	4	--	--	--	4	--	--	--
	HL–66–2	21.60, L, T	9	--	--	--	--	--	1	--	--	--	--	--	--	--	--
	HL–66–3	27.50, L. T	--	--	--	2	--	--	--	6	--	--	--	--	2	--	--
	HL–66–4A	33.00, L, Ss	--	--	--	2	--	--	2	3	--	--	--	3	--	--	--
	HL–66–4B	35.00, L, Ss	--	1	--	1	4	--	--	1	--	--	--	3	--	--	--
	HL–66–4C	41.00, L, Ss	--	--	Tr	--	5	--	--	2	--	--	--	2	--	--	1
	HL–66–5A	47.60, Uk, Ss	2	--	--	2	--	--	2	--	--	--	--	4	--	--	--
	HL–66–5B	49.30, Uk, T	--	--	--	1	6	--	--	2	--	--	--	--	--	1	--
	HL–66–7A	56.80, Uk, T	2	--	--	3	--	2	3	--	--	--	--	--	--	--	--
	HL–66–7B	57.70, Uk, T	2	--	--	3	1	--	4	--	--	--	--	--	--	--	--
	HL–66–7C	60.70, Uk, Ss	1	--	--	2	--	--	5	--	--	--	--	2	--	--	--
	HL–66–9	69.50, Uk, Ss	--	--	--	3	1	--	1	--	--	--	--	5	--	--	--
	HL–66–10	81.00, Uk, St	--	--	--	4	2	1	Tr	--	--	--	--	3	--	--	--
	HL–66–11A	92.50, Uk, T	--	--	--	3	1	--	--	--	--	--	--	--	--	6	--
	HL–66–11B	92.90, Uk, Ls	--	--	--	2	1	--	--	--	--	--	--	1	--	5	1
	HL–66–12	97.80, Uk, T	2	--	--	3	Tr	Tr	--	--	--	--	--	2	--	3	--

Locality No.	Sample No.	Sample location	Glass	Opal-CT	Mica	Smectite	Phil-lipsite	Chabazite	Erionite	Clinop-tilolite	Mordenite	Analcime	Potassium feldspar	Alkali feldspar	Quartz	Calcite	Other
69	HL–69A	U, T	--	--	--	1	--	--	--	9	--	--	--	--	--	Tr	--
	HL–69B	U, T	--	--	--	Tr	--	--	--	8	--	--	2	--	--	--	--
70	HL–70	U, T	--	--	--	1	--	--	1	8	--	--	--	--	--	--	--
71	HL–71	U, T	--	--	--	Tr	--	--	--	--	--	4	1	Tr	5	--	--
72	HL–72	U, T	--	--	--	1	--	Tr	Tr	5	--	--	--	4	--	--	--
73	HL–73	U, T	--	--	--	1	--	--	--	7	--	--	--	--	--	2	--
74	HL–74	U, T	--	--	--	--	--	--	Tr	10	--	--	--	--	--	--	--
75	HL–75A	U, Ls	--	--	--	1	--	--	--	1	--	--	--	1	--	7	--
	HL–75B	U, T	--	--	--	--	--	--	Tr	10	--	--	--	Tr	--	--	--
76	HL–76A	U, T	--	--	--	1	2	--	--	7	--	--	--	--	--	--	--
78	HL–78A	Tdc	--	1	--	--	--	--	--	8	--	--	--	1	--	--	--
	HL–78B	Tdc	--	--	--	--	--	--	Tr	7	--	--	--	3	--	--	--
79	HL–79A	Uk, T	--	3	--	--	--	--	--	7	--	--	--	--	--	--	--
	HL–79B	Uk, Ls	--	2	--	1	--	--	--	2	--	--	--	1	--	4	--
	HL–79C	Uk, T	--	1	--	--	--	--	--	3	6	--	--	--	--	--	--
80	HL–80	Uk, T	--	--	--	--	--	--	--	--	9	--	--	1	--	--	--
81	HL–81	L, T	3	--	--	1	--	--	4	--	--	--	--	1	--	1	--
82	HL–82	Tdc	4	--	--	--	--	3	Tr	--	--	--	--	3	Tr	--	--
83	HL–83A	U, T	2	--	--	1	--	--	5	--	--	--	--	1	--	1	--
	HL–83B	U, T	5	--	--	--	--	--	5	--	--	--	--	--	--	--	--
84	HL–84	Uk, T	--	--	--	--	--	--	2	8	--	--	--	--	--	Tr	--
85	HL–85A	Uk, Ss	--	--	--	Tr	--	--	4	2	--	--	--	3	--	1	--
	HL–85B	Uk, T	--	--	--	--	4	--	3	1	--	--	--	2	--	Tr	--
86	HL–86	U, T	--	--	--	1	--	--	--	6	--	--	--	--	3	--	--
87	HL–87B	Tdc	--	--	--	1	--	--	--	--	--	--	6	2	2	--	--
89	HL–89A	Uk, T	--	--	--	2	--	--	1	7	--	--	--	--	--	--	--
	HL–89B	Uk, T	--	--	--	1	--	--	--	4	--	2	--	--	3	--	--
90	HL–90A	Tpc	--	--	--	1	--	--	--	9	--	--	--	--	--	--	--
	HL–90B	Tpc	--	--	--	--	--	--	Tr	10	--	--	--	--	--	--	--

Appendix. Mineralogic composition of Miocene tuffaceous rocks near Harney Lake, Harney County, Oregon, as estimated from X-ray diffractometer patterns of bulk samples—Continued.

Locality No.	Sample No.	Sample location	Glass	Opal-CT	Mica	Smectite	Phil-lipsite	Chabazite	Erionite	Clinop-tilolite	Mordenite	Analcime	Potassium feldspar	Alkali feldspar	Quartz	Calcite	Other
91	HL–91A	Uk, T	--	--	--	1	--	--	--	8	--	--	--	--	1	--	--
	HL–91B	Uk, Ls	--	--	--	1	--	--	--	--	--	--	--	Tr	7	2	--
92	HL–92	Uk, T	--	--	--	3	--	--	--	1	--	3	--	--	3	Tr	--
93	HL–93	U, T	--	--	--	--	--	--	--	--	7	--	3	--	--	--	--
94	HL–94	Tpc	--	--	--	1	--	--	Tr	9	--	--	--	--	--	--	--
95	HL–95	Tdc	--	1	--	Tr	--	--	--	--	6	--	--	1	2	--	--
96	HL–96A	U, T	--	--	--	5	--	--	--	--	Tr	--	--	--	--	5	--
	HL–96B	U, Ls	--	--	--	--	--	--	--	--	--	--	--	--	8	2	--
97	HL–97	U, T	--	--	--	3	--	--	--	5	--	--	--	--	--	2	--
98	HL–98A	U, T	--	--	--	Tr	--	--	Tr	9	--	--	--	--	1	--	--
	HL–98B	U, T	--	--	--	--	--	--	Tr	8	--	--	--	--	2	--	--
99	HL–99A	U, T	--	2	--	--	4	--	--	3	--	--	--	1	--	--	--
	HL–99B	U, T	--	1	--	--	4	--	--	3	--	--	--	2	--	--	--
100	HL–100	U, T	--	--	--	1	--	6	3	--	--	--	--	Tr	--	--	--
101	HL–101	U, T	--	--	--	2	3	--	1	1	--	--	--	3	--	--	--
102	HL–102A	Tdc	6	--	--	Tr	--	--	1	--	--	--	--	3	Tr	--	--
	HL–102B	Tdc	4	--	--	1	--	--	1	--	--	--	--	3	1	--	--
103	HL–103A	U, T	6	--	--	2	--	--	--	--	--	--	--	2	Tr	--	--
	HL–103B	U, T	--	--	--	1	9	--	--	Tr	--	--	--	--	--	--	--
	HL–103C	Trs	8	--	--	2	--	--	--	--	--	--	--	Tr	Tr	--	--
104	HL–104	Trs	9	--	--	--	--	--	--	--	--	--	--	1	--	--	--
105	HL–105	Tdc	--	Tr	--	--	--	--	--	6	--	--	2	1	1	--	--
106	HL–106A	Tdc	6	--	--	--	--	2	--	Tr	--	--	--	1	1	--	--
	HL–106B	Tdc	--	1	--	--	6		1	Tr	--	--	--	1	1	--	--
107	HL–107A	U, Ss	--	--	--	3	3	--	--	1	--	--	--	3	--	--	--
	HL–107B	U, T	--	--	--	2	Tr	Tr	--	Tr	--	7	--	1	Tr	--	--
	HL–107C	U, Ss	--	--	--	2	--	--	2	2	--	--	--	3	1	--	Tr
110	HL–110A	Uk, T	--	--	--	2	--	--	--	8	--	--	--	Tr	Tr	--	--
	HL–110B	Uk, Ss	--	--	--	3	--	--	--	5	--	--	--	2	--	--	--

★U.S. GOVERNMENT PRINTING OFFICE: 1994–673–046/86066

SELECTED SERIES OF U.S. GEOLOGICAL SURVEY PUBLICATIONS

Periodicals

Earthquakes & Volcanoes (issued bimonthly).
Preliminary Determination of Epicenters (issued monthly).

Technical Books and Reports

Professional Papers are mainly comprehensive scientific reports of wide and lasting interest and importance to professional scientists and engineers. Included are reports on the results of resource studies and of topographic, hydrologic, and geologic investigations. They also include collections of related papers addressing different aspects of a single scientific topic.

Bulletins contain significant data and interpretations that are of lasting scientific interest but are generally more limited in scope or geographic coverage than Professional Papers. They include the results of resource studies and of geologic and topographic investigations; as well as collections of short papers related to a specific topic.

Water-Supply Papers are comprehensive reports that present significant interpretive results of hydrologic investigations of wide interest to professional geologists, hydrologists, and engineers. The series covers investigations in all phases of hydrology, including hydrogeology, availability of water, quality of water, and use of water.

Circulars present administrative information or important scientific information of wide popular interest in a format designed for distribution at no cost to the public. Information is usually of short-term interest.

Water-Resources Investigations Reports are papers of an interpretive nature made available to the public outside the formal USGS publications series. Copies are reproduced on request unlike formal USGS publications, and they are also available for public inspection at depositories indicated in USGS catalogs.

Open-File Reports include unpublished manuscript reports, maps, and other material that are made available for public consultation at depositories. They are a nonpermanent form of publication that may be cited in other publications as sources of information.

Maps

Geologic Quadrangle Maps are multicolor geologic maps on topographic bases in 7 1/2- or 15-minute quadrangle formats (scales mainly 1:24,000 or 1:62,500) showing bedrock, surficial, or engineering geology. Maps generally include brief texts; some maps include structure and columnar sections only.

Geophysical Investigations Maps are on topographic or planimetric bases at various scales; they show results of surveys using geophysical techniques, such as gravity, magnetic, seismic, or radioactivity, which reflect subsurface structures that are of economic or geologic significance. Many maps include correlations with the geology.

Miscellaneous Investigations Series Maps are on planimetric or topographic bases of regular and irregular areas at various scales; they present a wide variety of format and subject matter. The series also includes 7 1/2-minute quadrangle photogeologic maps on planimetric bases which show geology as interpreted from aerial photographs. Series also includes maps of Mars and the Moon.

Coal Investigations Maps are geologic maps on topographic or planimetric bases at various scales showing bedrock or surficial geology, stratigraphy, and structural relations in certain coal-resource areas.

Oil and Gas Investigations Charts show stratigraphic information for certain oil and gas fields and other areas having petroleum potential.

Miscellaneous Field Studies Maps are multicolor or black-and-white maps on topographic or planimetric bases on quadrangle or irregular areas at various scales. Pre-1971 maps show bedrock geology in relation to specific mining or mineral-deposit problems; post-1971 maps are primarily black-and-white maps on various subjects such as environmental studies or wilderness mineral investigations.

Hydrologic Investigations Atlases are multicolored or black-and-white maps on topographic or planimetric bases presenting a wide range of geohydrologic data of both regular and irregular areas; principal scale is 1:24,000 and regional studies are at 1:250,000 scale or smaller.

Catalogs

Permanent catalogs, as well as some others, giving comprehensive listings of U.S. Geological Survey publications are available under the conditions indicated below from the U.S. Geological Survey, Books and Open-File Reports Section, Federal Center, Box 25425, Denver, CO 80225. (See latest Price and Availability List.)

"Publications of the Geological Survey, 1879-1961" may be purchased by mail and over the counter in paperback book form and as a set of microfiche.

"Publications of the Geological Survey, 1962-1970" may be purchased by mail and over the counter in paperback book form and as a set of microfiche.

"Publications of the U.S. Geological Survey, 1971-1981" may be purchased by mail and over the counter in paperback book form (two volumes, publications listing and index) and as a set of microfiche.

Supplements for 1982, 1983, 1984, 1985, 1986, and for subsequent years since the last permanent catalog may be purchased by mail and over the counter in paperback book form.

State catalogs, "List of U.S. Geological Survey Geologic and Water-Supply Reports and Maps For (State)," may be purchased by mail and over the counter in paperback booklet form only.

"Price and Availability List of U.S. Geological Survey Publications," issued annually, is available free of charge in paperback booklet form only.

Selected copies of a monthly catalog "New Publications of the U.S. Geological Survey" available free of charge by mail or may be obtained over the counter in paperback booklet form only. Those wishing a free subscription to the monthly catalog "New Publications of the U.S. Geological Survey" should write to the U.S. Geological Survey, 582 National Center, Reston, VA 22092.

Note.--Prices of Government publications listed in older catalogs, announcements, and publications may be incorrect. Therefore, the prices charged may differ from the prices in catalogs, announcements, and publications.